R76-29

FEBRUARY 1976

TECHNICAL REPORT ON THE

ELECTROMECHANICAL FLIGHT CONTROL ACTUATOR

CONTRACT NAS 9-14331

Submitted to

NATIONAL AERONAUTICS and SPACE ADMINISTRATION

L.B. Johnson Space Center

Houston, Texas

Delco Electronics

General Motors Corporation
- Santa Barbara Operations
Santa Barbara, California

R76-29

FEBRUARY 1976

TECHNICAL REPORT ON THE

ELECTROMECHANICAL FLIGHT CONTROL ACTUATOR

CONTRACT NAS 9-14331

Submitted to

NATIONAL AERONAUTICS and SPACE ADMINISTRATION

L.B. Johnson Space Center

Houston, Texas

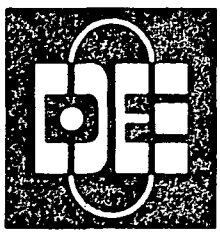

Delco Electronics

General Motors Corporation
- Santa Barbara Operations
Santa Barbara, California

CONTENTS

ILLUSTRATIONS

TABLES

SECTION I
INTRODUCTION

The present Space Shuttle flight control system uses actuators powered by a hydraulic system similar to conventional large aircraft hydraulic systems. This system is heavy, relatively inefficient, and requires a large energy source and thermal control system. Weight reduction programs have initiated studies that indicate a highly efficient battery-powered electromechanical actuator system could significantly reduce Shuttle weight. However, hardware feasibility has not been demonstrated for the electromechanical actuator concepts considered to be candidates for the Shuttle application.

The purpose of the Electromechanical Flight Control Actuator Program is to develop an electromechanical actuator that will follow a proportional control command with minimum wasted energy, and demonstrate the feasibility of meeting space vehicle actuator requirements using advanced electromechanical concepts.

The electromechanical actuator development program includes the following tasks:

- Design and Analysis
- Fabrication and Assembly
- Testing
- Reports and Data.

The design and analysis task has been accomplished under an on-going Delco-funded development program. The remaining efforts have been conducted under NASA/JSC contract NAS 9-14331.

Acknowledgments

Although a number of individuals have made significant contributions to this program, the efforts of several key personnel merit special recognition. Messrs. B. Nikodemski and F. Bourbeau were instrumental in the electronics design, Mr. E. Sawyer was largely responsible for the motor design, Mr. W. Gully contributed to the mechanical design, and Mr. B. Meredith has been largely responsible for fabrication of the electronic equipment.

SECTION II
SUMMARY

2.1 SYSTEM REQUIREMENTS

The requirements for the electromechanical actuator were established in the program Statement of Work*. Some of the more important design goals are summarized in Table 2-1.

	DESIGN GOALS
OUTPUT STROKE	55 DEGREES (+15, -40 DEGREES)
OUTPUT VELOCITY/TORQUE	20 DEGREES/SECOND AT 0.357×10^6 in-lb 15 DEGREES/SECOND AT 0.539×10^6 in-lb
FREQUENCY RESPONSE	3 HZ AT 1^0 PP AT 0.300×10^6 in-lb HM 1 HZ AT 4^0 PP AT 0.140×10^6 in-lb HM
DISPLACEMENT LINEARITY	1.0% FULL TRAVEL (FT)
THRESHOLD	0.01% INPUT SIGNAL TO ACHIEVE 100% FT
POSITION NULL	0.5% FT
HYSTERESIS	0.005% FT
VELOCITY TRACKING	3% OF MAXIMUM MOTOR VELOCITY
MOTOR BRAKE RELEASE	10 ms
CHATTER AND INSTABILITY	0.055 DEGREES PP

Table 2-1. EM Actuator Performance Requirements

*Statement of Work for Electromechanical Actuator, NASA L. B. Johnson Space Center, Houston, Texas, August 2, 1974.

2.2 EQUIPMENT STATUS

The electromechanical actuator design is essentially complete. Status of the various major subsystems is given in Table 2-2.

Major Subsystem	Design	Fabrication	Assembly
Differential Gearbox Assembly	Complete	Complete	Complete; re-shimming may be done later to minimize back lash.
Motor/Brake Assembly	Complete	Fabrication complete for five motors; one set of motor parts to be used as spares.	1. Motors 1 and 2 need brake springs and stator sleeves installed. 2. Motors 3 and 4 need brake assembly, stator sleeve and tachometer couplings installed. 3. The coupling design should be changed to improve its torsional stiffness; a bellows type coupling has been purchased for this purpose, and some minor design changes will be required.
Control Electronics-Start-Up Shut-Down, and Main Power	Complete	Complete	Complete
Control Electronics-Low-Level Electronics	Complete	Complete	1. The fourth channel has not been wired. 2. System gains and compensation techniques not finalized.
Control Electronics Power Electronics	Complete	Complete	Components for the fourth channel have been mounted on the heatsink, but the power supply and power wiring are not done.
Thermal Control System	Complete	Complete	Interconnecting hydraulic lines have not been installed, and the wiring is incomplete.

Table 2-2. Status of EM Actuator Major Subsystems

2.3 TEST RESULTS AND STATUS

Only single channel testing has been done thus far. These tests have been run with current limiting set at 40 A and with a battery voltage of 110 V. Relatively low system gains have been used in these tests, but the basic performance with respect to such characteristics as threshold and hysteresis has been very encouraging. Preliminary test results are sum-

marized in Table 2-3. It is expected that system performance will be improved as the system gains are increased.

PARAMETER	MEASURED	REQUIREMENT	DESIGN GOAL
THRESHOLD	0.02 deg	0.055 deg	0.0275 deg
POSITION NULL	0.02 deg		0.275 deg
LINEARITY	0.4 deg	0.55 deg	
ACCURACY	0.6 deg	1.1 deg	
HYSTERESIS	± 0.008 deg	0.055 deg	0.0275 deg

Table 2-3. Preliminary Test Results

Figure 2-1 summarizes test data taken during tests of the Delco breadboard system. The maximum torque-speed condition represents an output of 15.1 hp. The efficiency curve shown does not take into account such losses as those of the power supplies, pump, and indicators which receive power from the 60 Hz utility line. The efficiency was calculated by taking the ratio of the mechanical output power to the power supplied by the battery.

2.4 CONCLUSIONS AND RECOMMENDATIONS

As a near-term effort, the EM actuator hardware should be completed, the system gains and compensation methods should be optimized to achieve the required system performance, and system-level tests should be conducted. These tasks are necessary to lay the groundwork for the design of a prototype system.

Other related activities should include:

- Development and confirmation of system math models
- Redundancy management studies
- Power electronics improvement
- Motor improvement (particularly tachometer coupling)
- Load stand improvement (rigidizing).

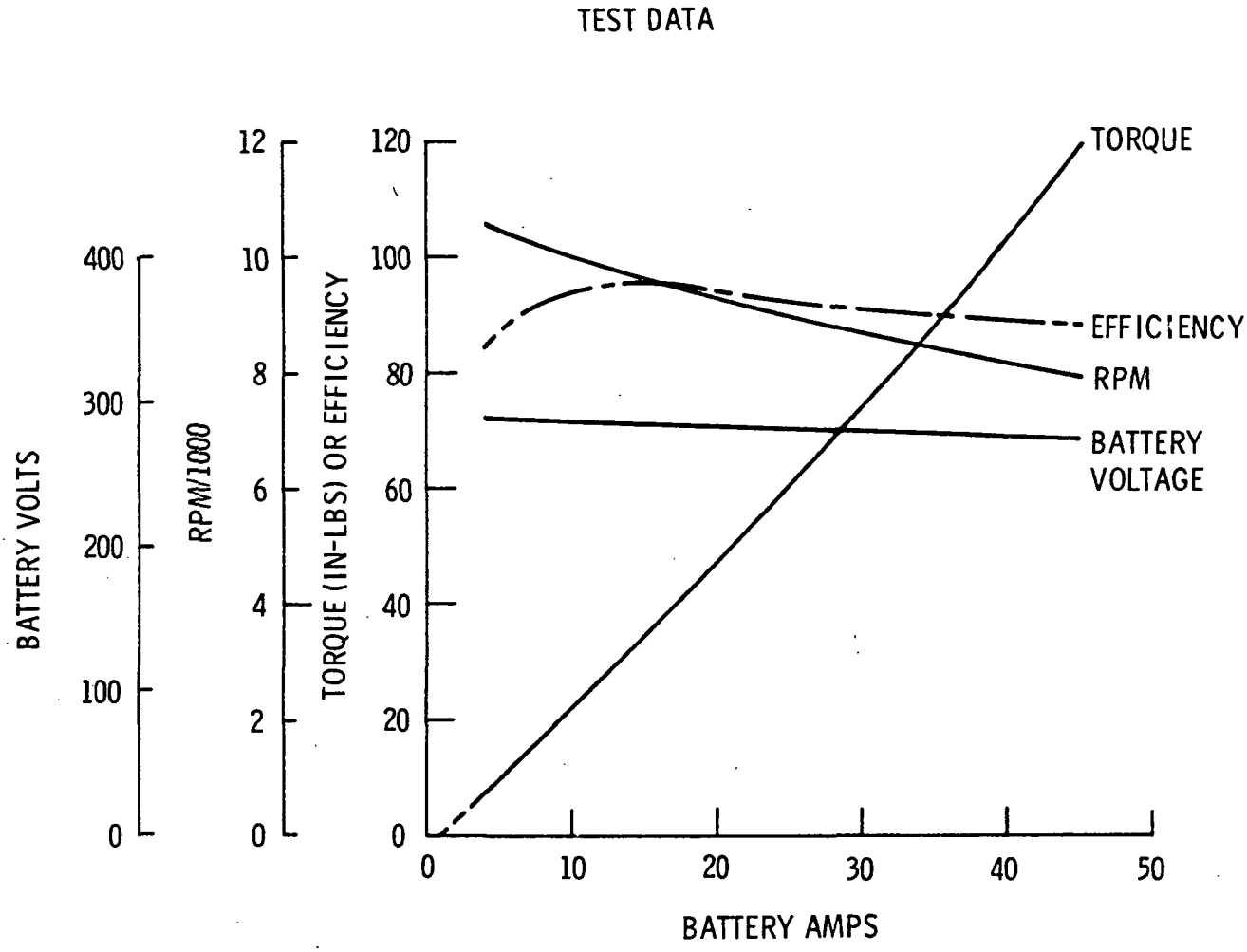

Figure 2-1. Test Data from Delco Breadboard System

SECTION III
SYSTEM FUNCTIONAL DESCRIPTION

3.1 GENERAL

The electromechanical actuator (Figure 3-1) is composed of four independent servo-controlled channels. Each channel consists of control and drive electronics, a brushless electric motor with brake, and velocity and position feedback transducers. The four electric motors are driven into a differential gearbox which has a common double-ended output which is coupled to the NASA-supplied rotary actuators. The output velocity of the gearbox is proportional to the sum of the velocities of the motors. In the normal mode of operation, two of the four motors are driving and the other two are braked. Each motor has independent control and drive electronics, providing servo control and power control for motoring and electrical braking modes of operation. The electromechanical actuator is powered from a battery which has a nominal terminal voltage of 270 V. The motors are brushless, self-synchronous machines with permanent-magnet rotors. They are controlled by solid-state electronics.

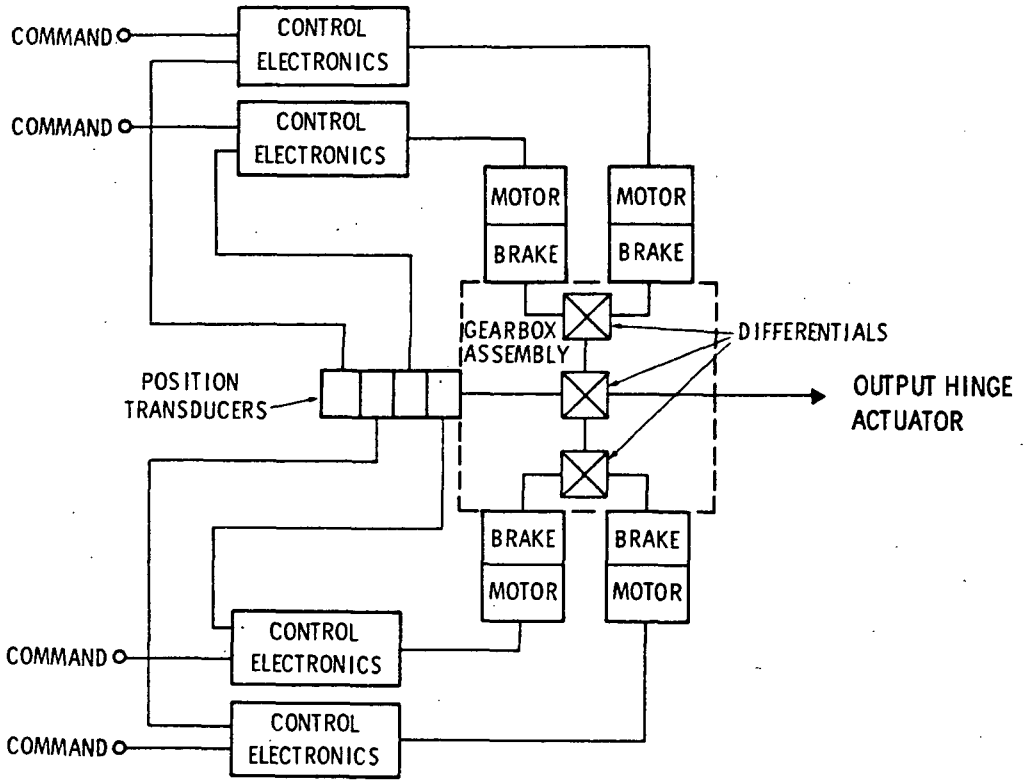

Figure 3-1. EM Actuator Block Diagram

3.2 SYSTEM OPERATION

Figure 3-2 is a simplified system block diagram of a single channel of the EM actuator. For convenience, all torque, inertia, and motion variables are referenced to the load. Linearized load effects (viscous damping, load spring and steady-state hinge moments) are represented, and the velocity and position feedback paths are shown.

The position command and position feedback signals are compared to form a position error signal. This signal is amplified and combined with the velocity feedback signal to develop a current command signal. The current source develops a motor current in response to the current command signal. The motor current produces a torque which accelerates the reflected inertia of the system and overcomes the reflected hinge moment of the load.

In normal operation, two channels of the EM actuator are active(Figure 3-3). Each motor is controlled in essentially the manner described in the preceding paragraphs, but a velocity correction loop is also included. The tachometer outputs of the two active channels are compared to form a velocity error signal. If the two motors are not rotating at the same angular velocity, the error signal causes the slower motor to speed up, and the faster motor to slow down. In this manner, under idealized operation, each motor would operate at the same speed, produce the same torque, and thus share the load equally with the other motor.

The servo aspects of the EM actuator design are given in Appendix A.

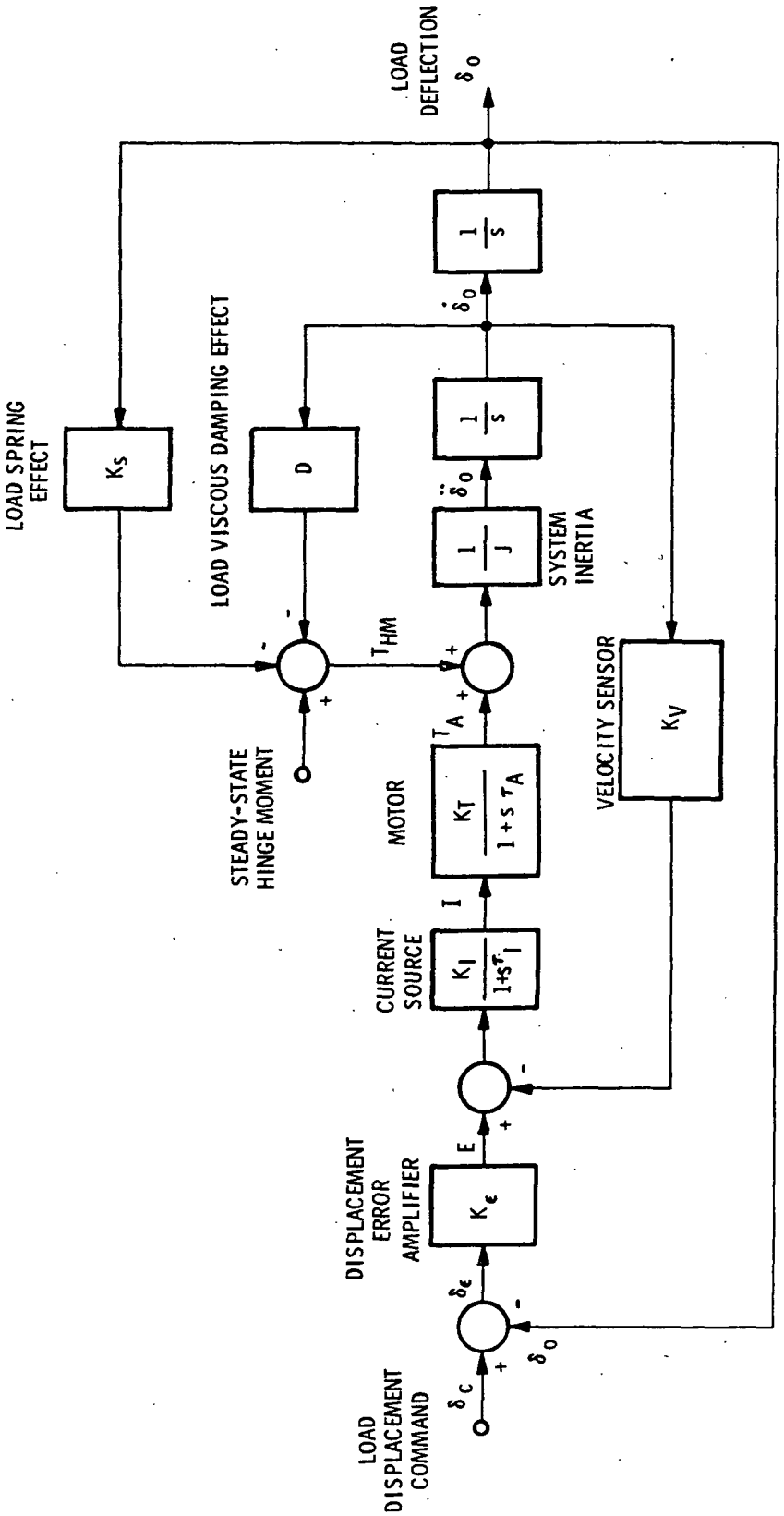

Figure 3-2. Simplified System Diagram, Single Channel

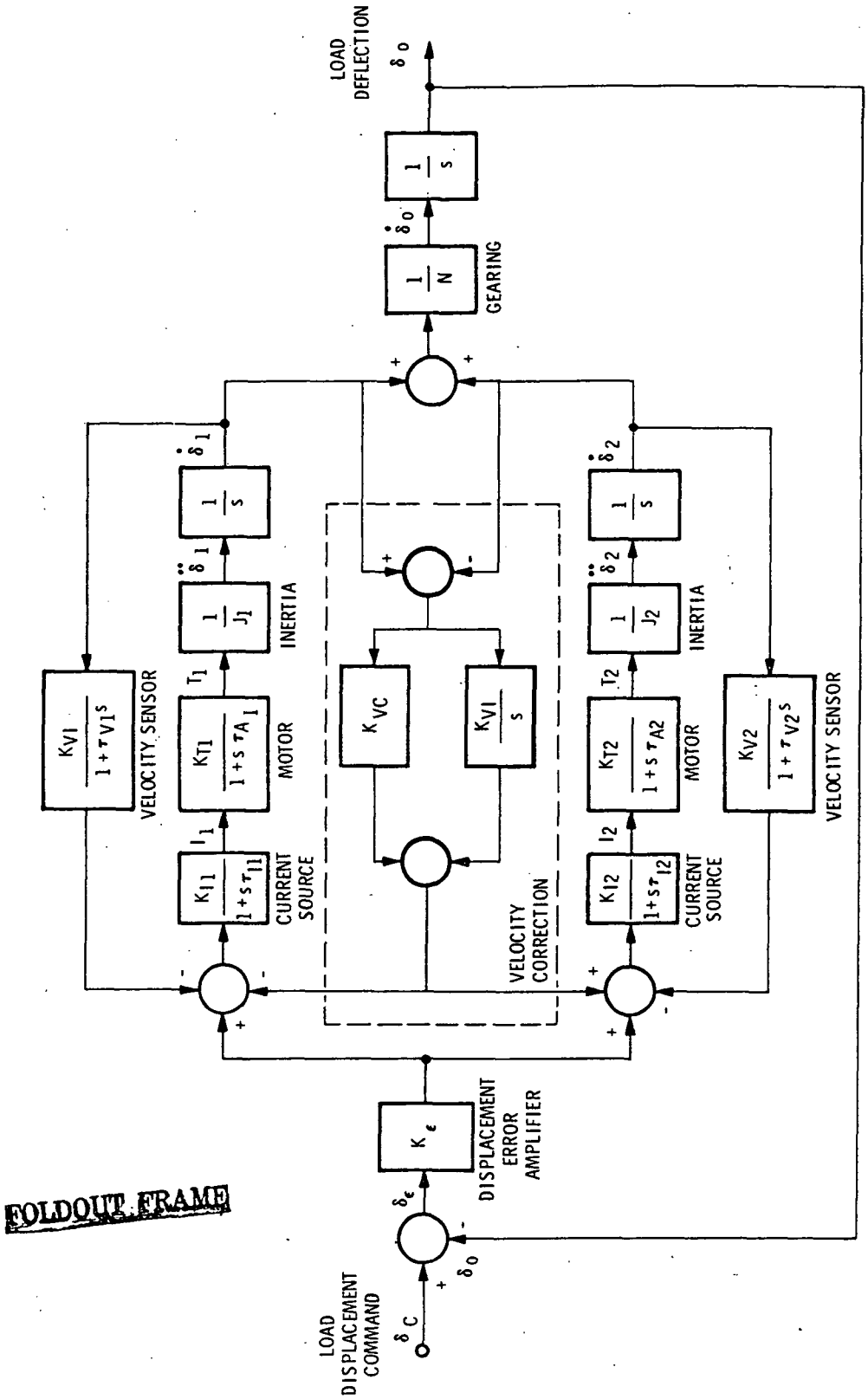

FOLDOUT FRAME

Figure 3-3. Two Channel Functional Diagram - Simplified

SECTION IV
EQUIPMENT DESCRIPTION

4.1 DELCO BREADBOARD SYSTEM*

4.1.1 POWER SOURCE

As indicated in Section III, the high voltage electrical power for the EM actuator is obtained from a battery (270V nominal). For development purposes, Delco utilized a battery bank consisting of 24 heavy duty batteries (Figure 4-1). Quick-disconnect cables were used to allow the battery voltage to be tapped at selected levels. The battery is connected through cables and protective switchgear to the Electromechanical Actuator Development Laboratory which is located approximately 150 feet from the battery bank. The batteries power both the Delco breadboard and the NASA four-channel actuator system.

Figure 4-2 shows the battery charger which was used with the system. A simple Variac control was used to adjust the charger output voltage and control the battery charging rates.

4.1.2 SYSTEM DESCRIPTION

The Delco breadboard system consists of a single channel of electronics, a motor, a gear train, and position and velocity feedback transducers. The assembly which was used in developing the basic circuitry for the electromechanical actuator is shown in Figure 4-3. The electronics rack includes a variety of instrumentation used to monitor motor currents and various system voltages. Torque transducer and r/min instrumentation is also mounted in the rack along with an electronic wattmeter. The electromechanical assembly (Figure 4-4) is mounted on the laboratory bench and consists of a baseplate on which are fastened the synchronous motor, dynamometer, gear train and associated electromechanical assemblies. At this stage of the program, the permanent magnet motor had not yet been developed; the actuator motor shown in the lower right-hand corner of Figure 4-4 is a five kilowatt wound-rotor, self-synchronous motor which is operated with fixed field excitation. The motor is coupled to a torque transducer which also provides an r/min indication by means of a toothed wheel and permanent magnet pulse generator arrangement. The motor assembly is coupled to the large induction machine by means of a V-belt.

*The Delco breadboard system was used during the company-funded design development phase.

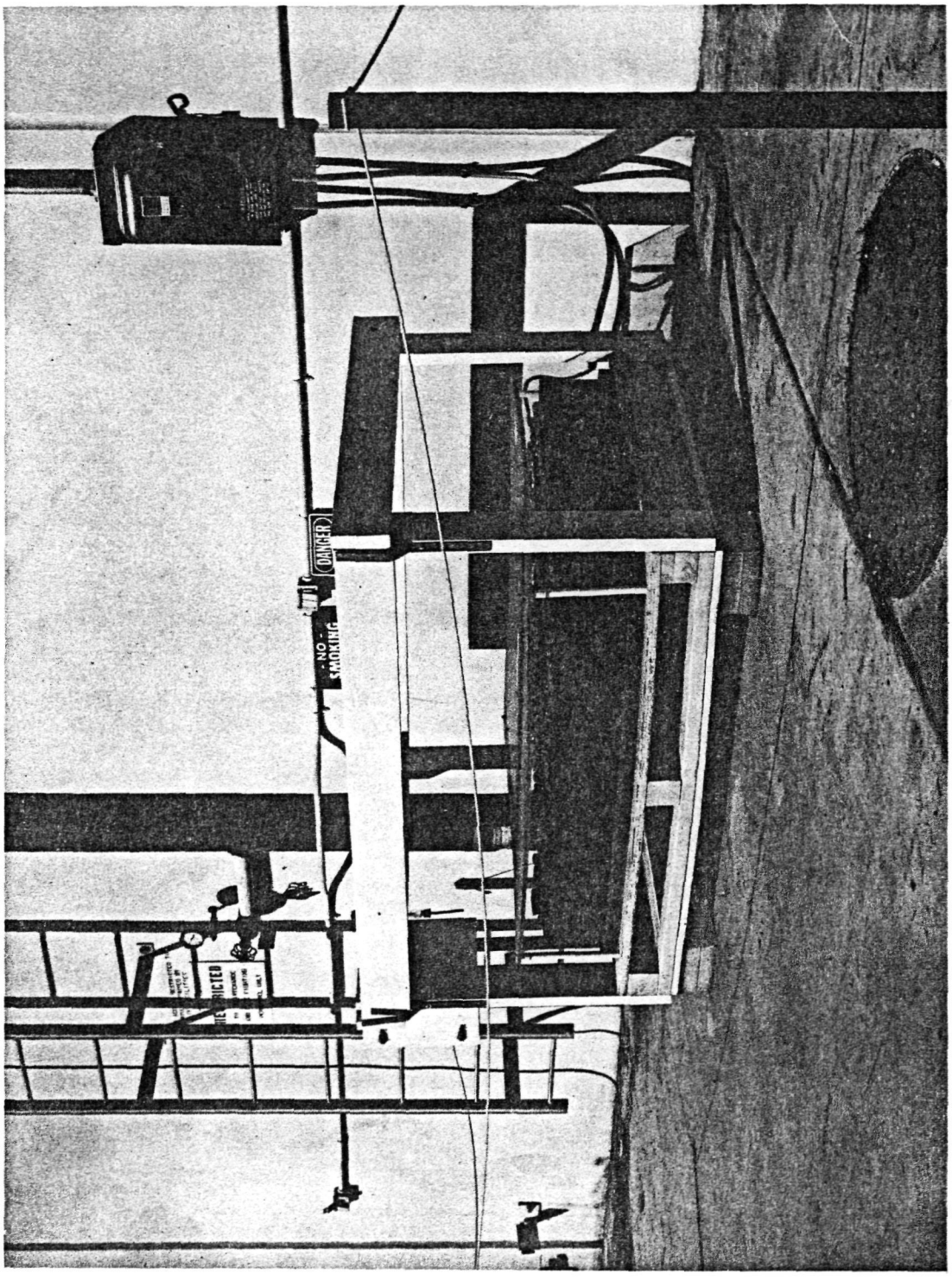

Figure 4-1. Battery Bank

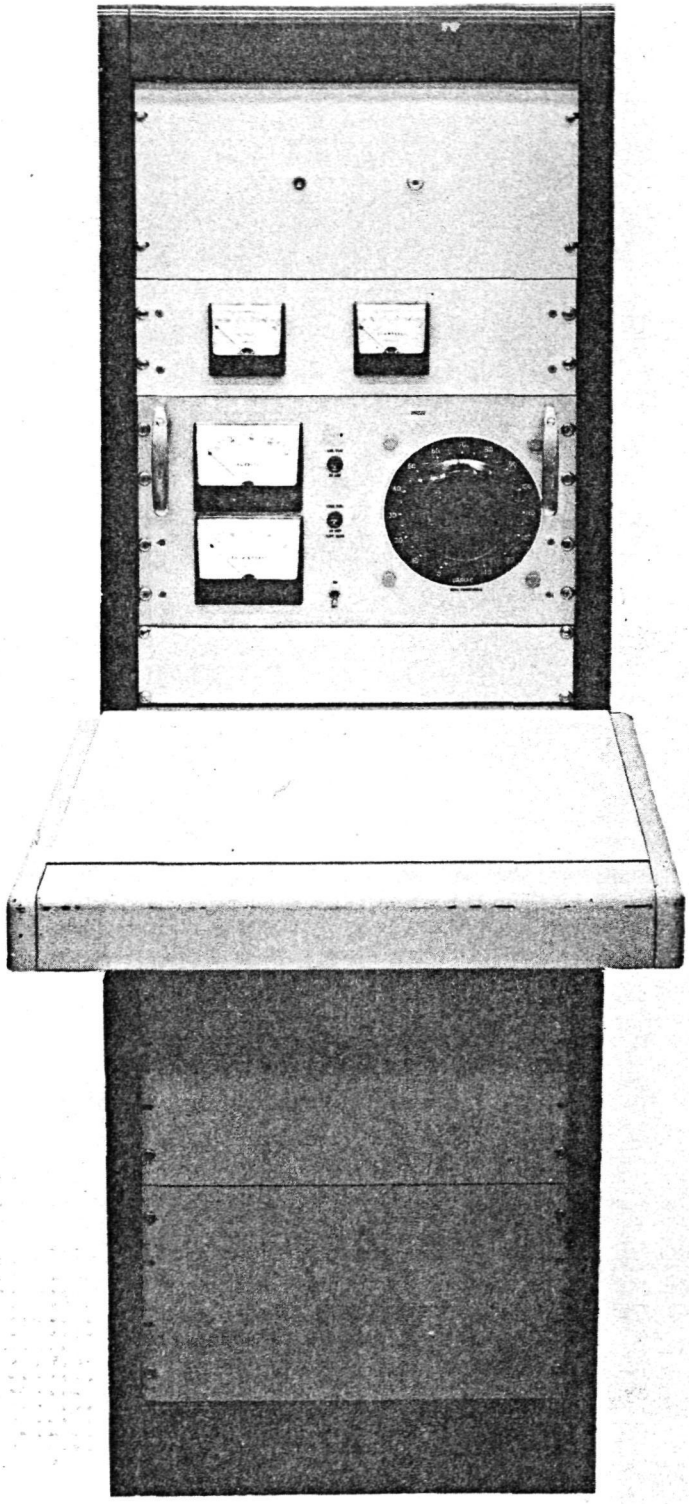

Figure 4-2. Battery Charger

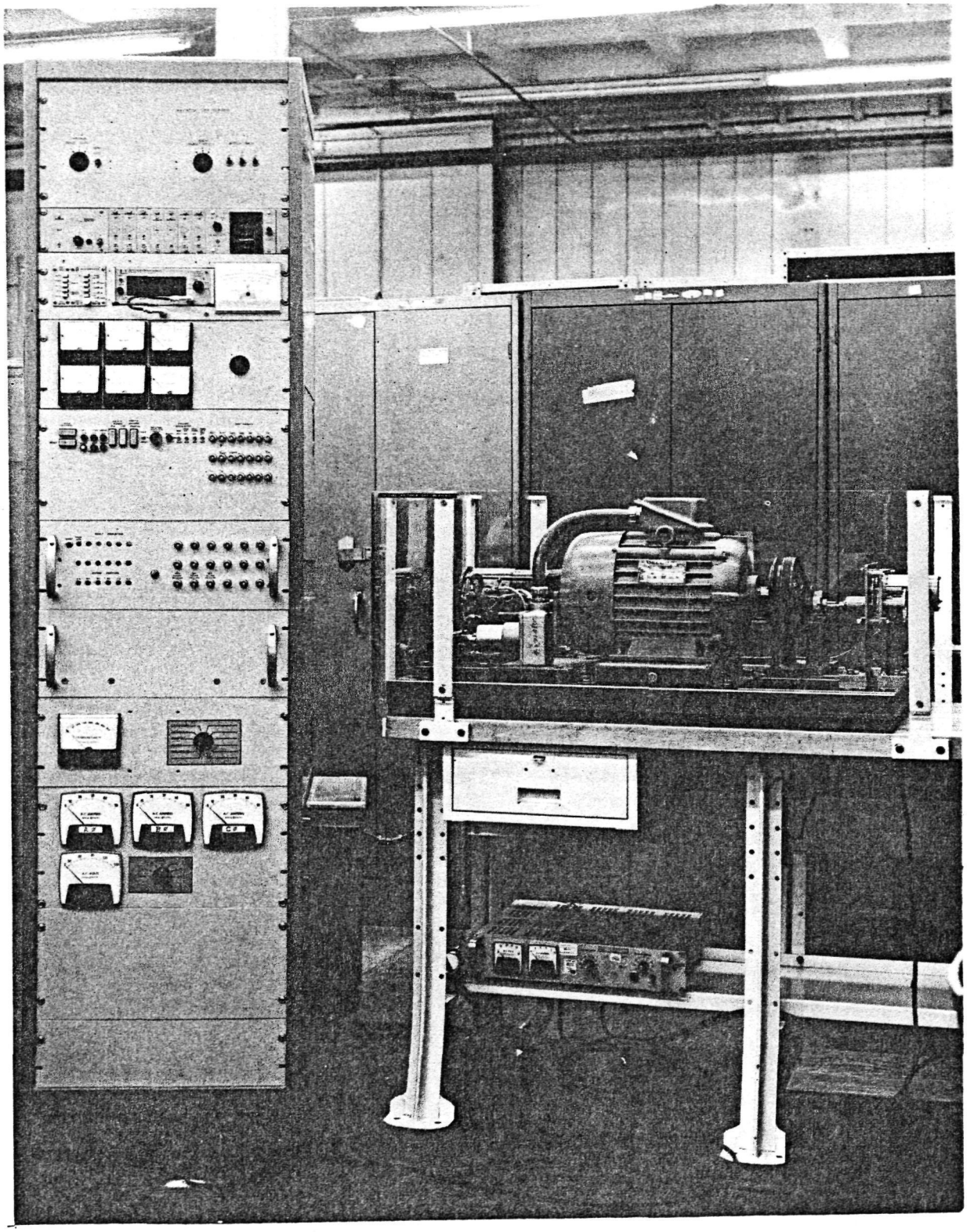

Figure 4-3. Delco Breadboard System

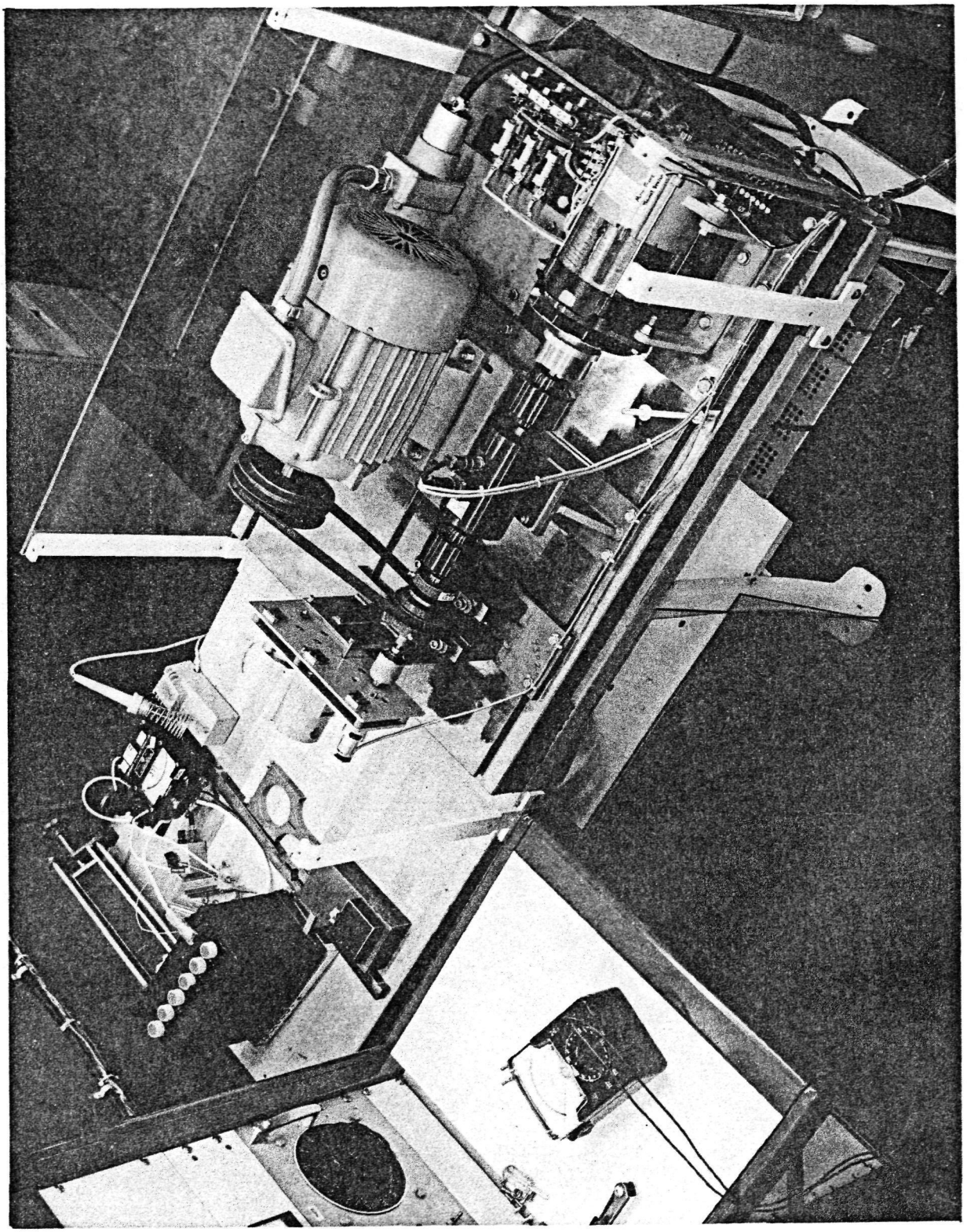

Figure 4-4. Delco Electromechanical Assembly

The induction motor was used to drive the assembly (when the actuator motor was operating as a generator), and it was also used as a dynamometer when the actuator was under test in its motoring mode.

The system also drives a servo-type gear reducer which is mounted at the left end of the baseplate. The gear reducer drives a tachometer at the high speed end and a position transducer potentiometer at the low speed end of the gear train. This arrangement was used to aid in system development before the final motor was designed. After the permanent magnet motor was designed, it was incorporated in the same basic breadboard assembly as shown in Figure 4-5. Here, a dc machine, coupled to the EM actuator by means of a toothed belt, is used to load or drive the actuator system. The dc machine's field and armature circuits were available for loading and control purposes. When operated as a generator, the dc machine supplied power to a resistive load bank.

4.2 NASA FOUR-CHANNEL SYSTEM

The four-channel motor/gearbox assembly was mounted on the NASA-developed test stand (Figure 4-6) which consists of two large spring assemblies located at each end of the stand. The springs are coupled by means of a clevis arm into the rotating portion of the stand. A 238.71:1 gear reducer is used to reduce the gearbox output speed to that of the simulated control surface motion. The gearbox and four motors are shown in Figure 4-6; at the time this picture was taken, there were two active channels connected to the power electronics. An air cooling system was in use for removing heat from the motors.

Figure 4-7 is a close-up view of the motor/gearbox assembly, and clearly shows the position feedback potentiometer and the torque tube which connects the gearbox output to the load stand.

4.2.1 DIFFERENTIAL GEARBOX

4.2.1.1 Power Train

The differential gearbox sums the velocities of the individual servo motors and provides a common output shaft. The gearbox also furnishes the required gear reduction ratio between the motor shaft and the rotary hinge actuator. A schematic of the system is shown in Figure 4-8.

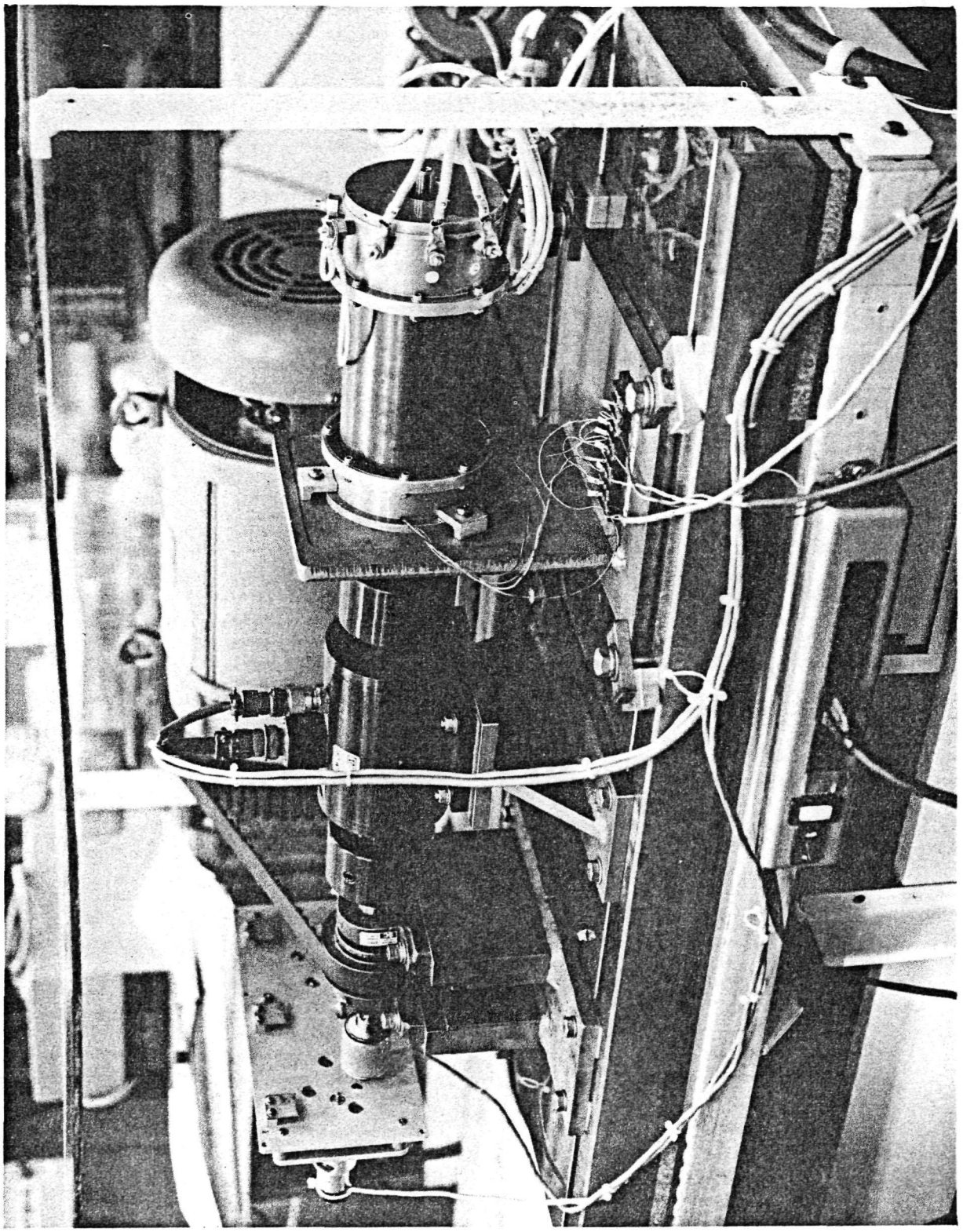

Figure 4-5. Delco Electromechanical Assembly

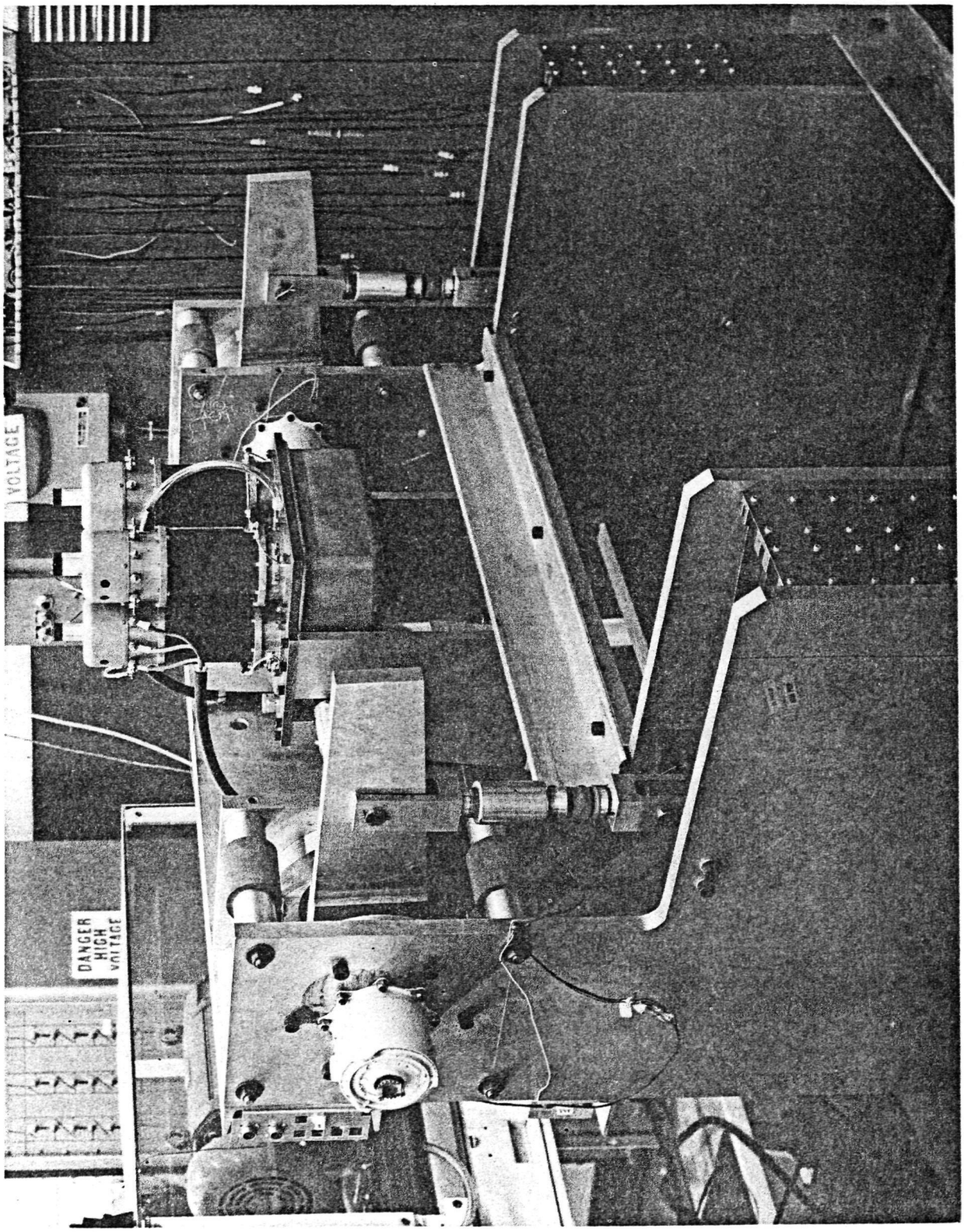

Figure 4-6. NASA Test Stand

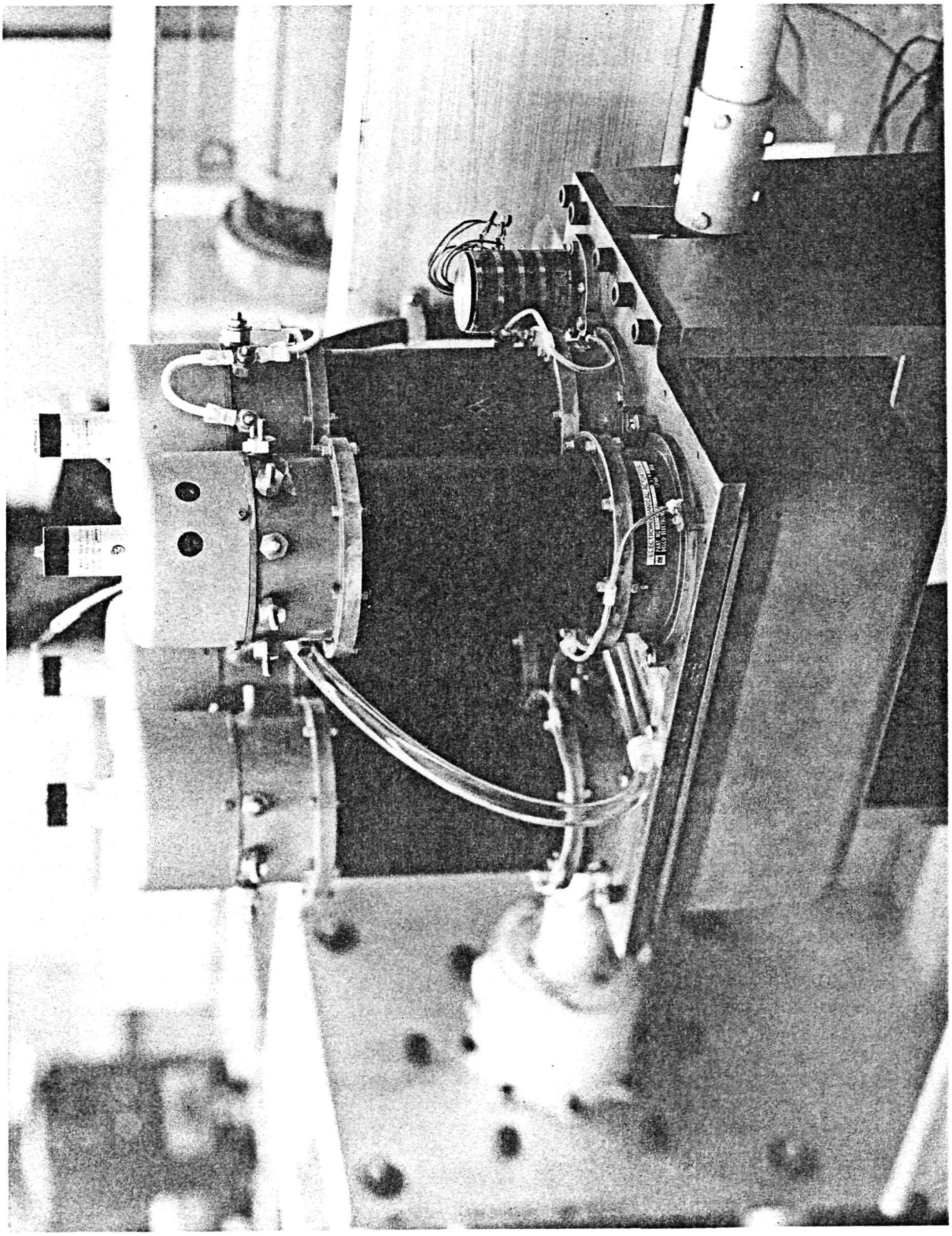

Figure 4-7. Motor/Gearbox

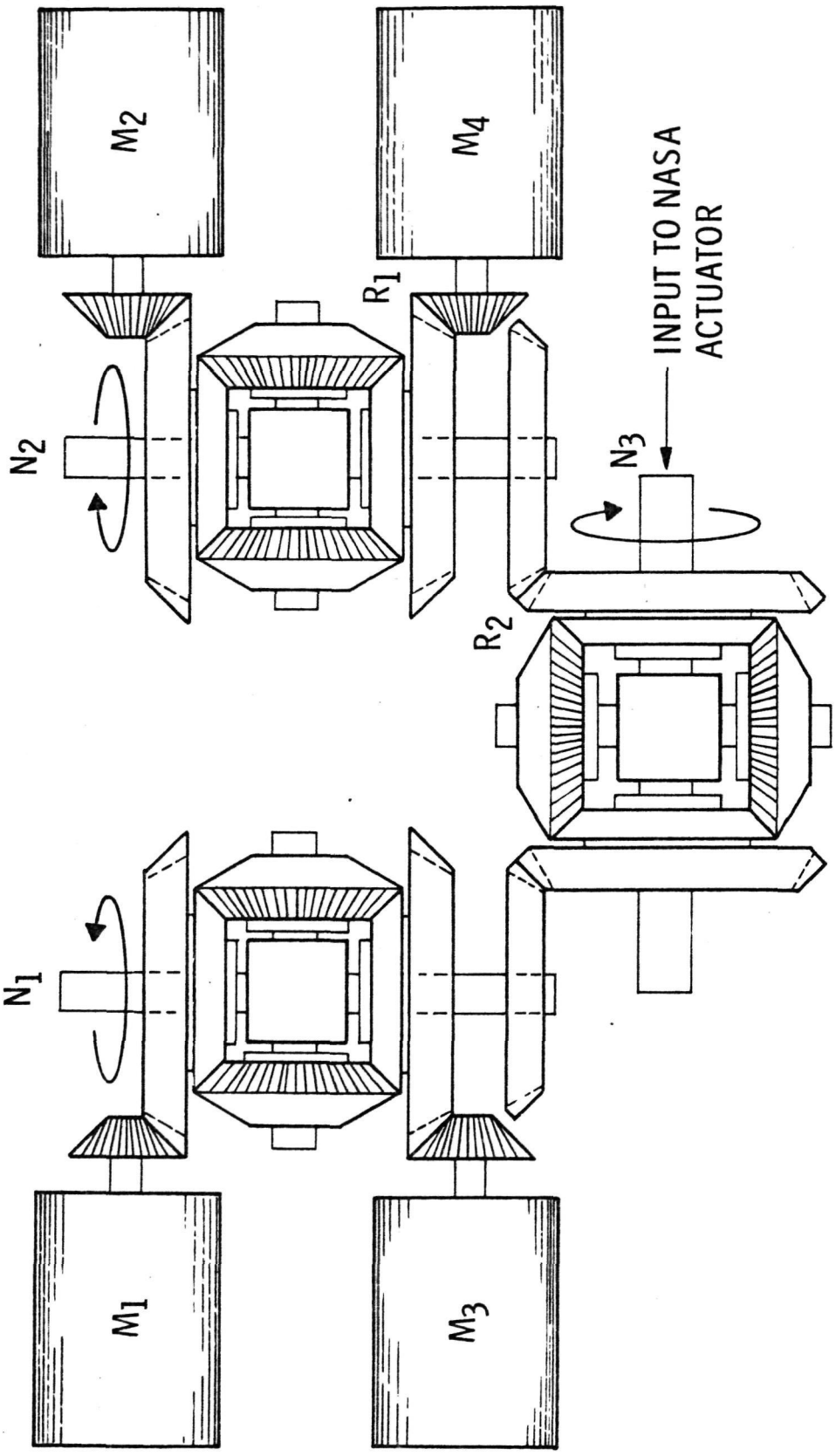

Figure 4-8. Differential Gearbox Arrangement

The maximum motor speed is approximately 9000 r/min and the overall gear reduction ratio is about 2700:1, resulting in a control surface rate of 20 degrees/s. Since the rotary hinge actuator (not part of the differential gearbox) reduction is 238.71:1, the differential gearing must provide a reduction of about 11.30:1.

When any two of the four motors are operating, the differential gear arrangement inherently has a 2:1 reduction; therefore, only a 5.65:1 additional gear reduction is required. This is accomplished in two stages: 3.75:1 between the motors and the first stage differential inputs, and 1.5:1 between the first and second stage differential inputs. By applying the larger reduction at the motor, the moment of inertia effect of the gear train is minimized.

4.2.1.2 Position Transducer Gear Train

The position transducer is coupled to the output of the EM actuator gearbox by means of precision servo gearing (The mounting hole for the position transducer assembly can be seen in the lower left hand corner of Figure 4-11). A worm gear (shown in Figure 4-11) drives an anti-backlash gear which is mounted on the position transducer shaft. The gear ratio of this train provides 5.189 degrees of position transducer motion for each degree of load motion (based on a gear reduction of 238.71:1 in the NASA-furnished rotary hinge actuator). With typical adjustment, the position transducer motion as a function of load angle would be as illustrated in Figure 4-9.

4.2.1.3 Position Transducer

The position transducer consists of four precision servo potentiometers ganged on a single shaft. The transducers utilize a film resistive element to achieve virtually infinite resolution. Some of the major features of the position transducer are:

Diameter	2.0 in
Resistance (each element)	20k ohms
Linearity	0.25%
Electrical Travel	340°
Standard Life Expectancy	10 M revolutions

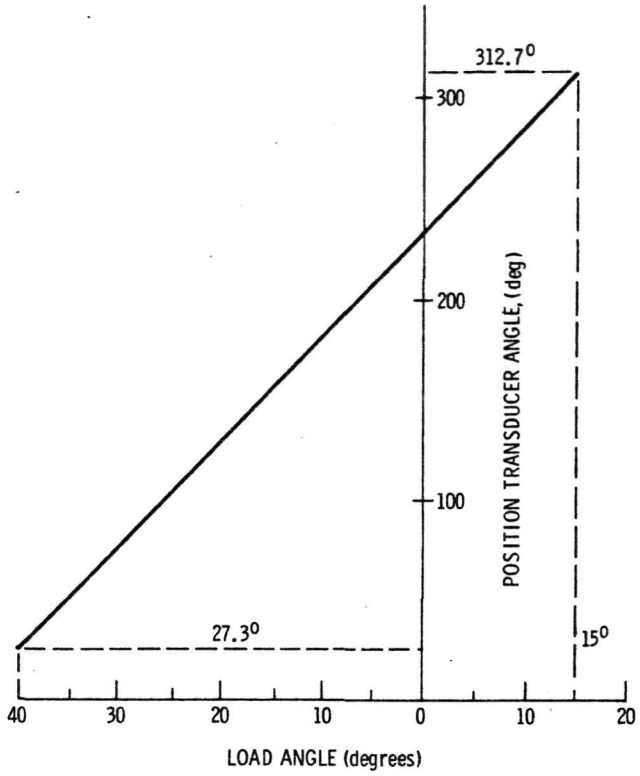

Figure 4-9. Position Transducer Motion

4.2.1.4 Physical Characteristics

The differential gearbox assembly (Figure 4-10) consists of three identical bevel gear differentials of the type often used in precision instruments. Input rotations are applied to the gears at either end of the bevel gear set. The output speed is taken off the "spider" or cage shaft.

The differential gear assembly is shown in Figure 4-11. All gears are ground spiral bevel gears specifically developed for this application and fabricated from high-quality gear steel as recommended by AGMA standards. "Zerol" spiral bevel gears (spiral gears with zero spiral angle) have been selected for this design to provide smooth operation, continuous pitch line contact, superior performance with low number of pinion teeth, and low axial bearing loads. Adjustment capability is provided to control gear mesh clearance and backlash. Basic gear sizing along with gear and pinion bending and contact stresses have been determined by the Gleason Works (See Appendix B for detailed gear data). Antifriction bearings of instrument quality are used throughout. Angular contact bearings have been chosen for uses when both axial and radial loads are present.

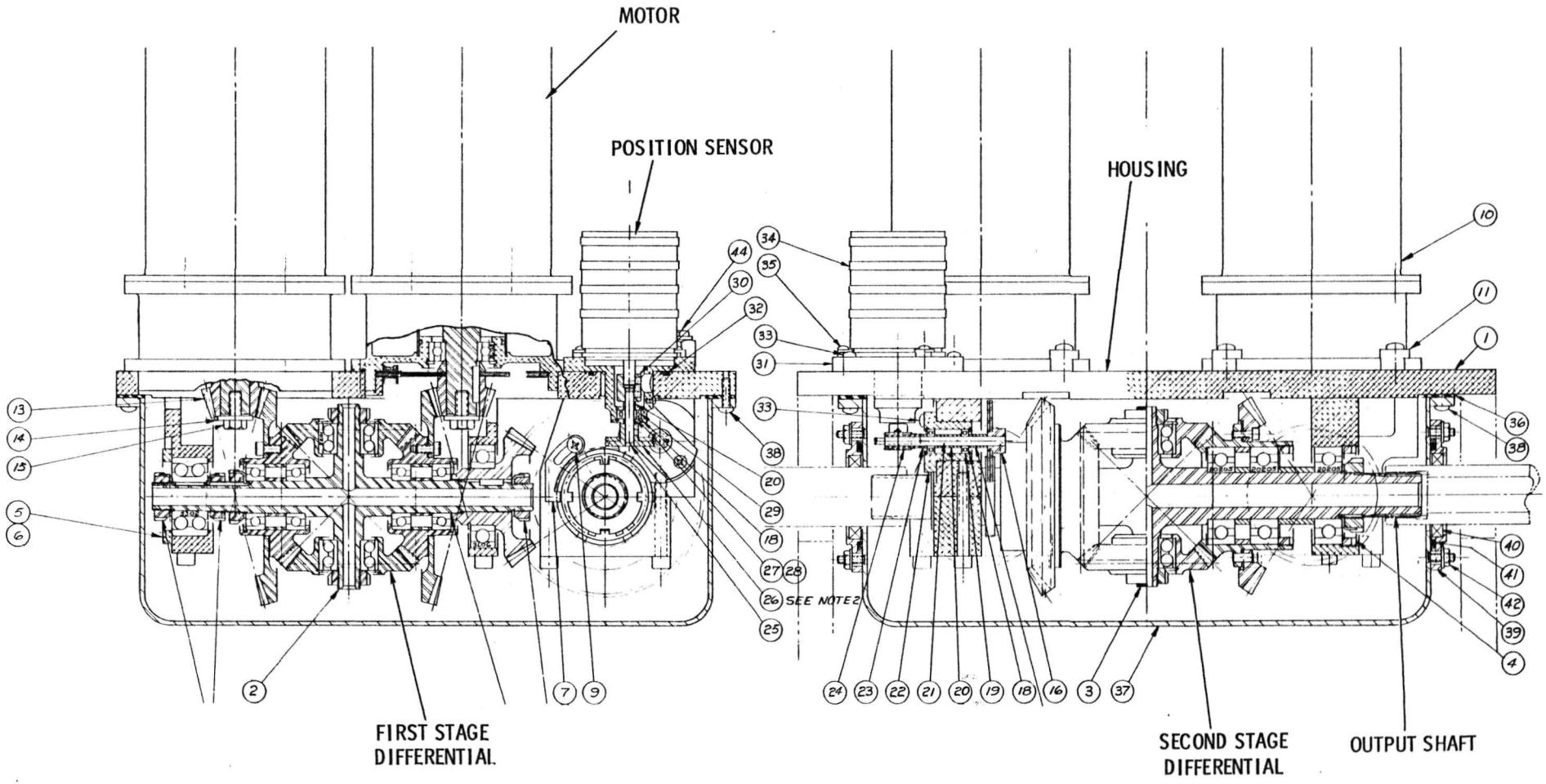

Figure 4-10. Four-Channel EM Actuator Assembly

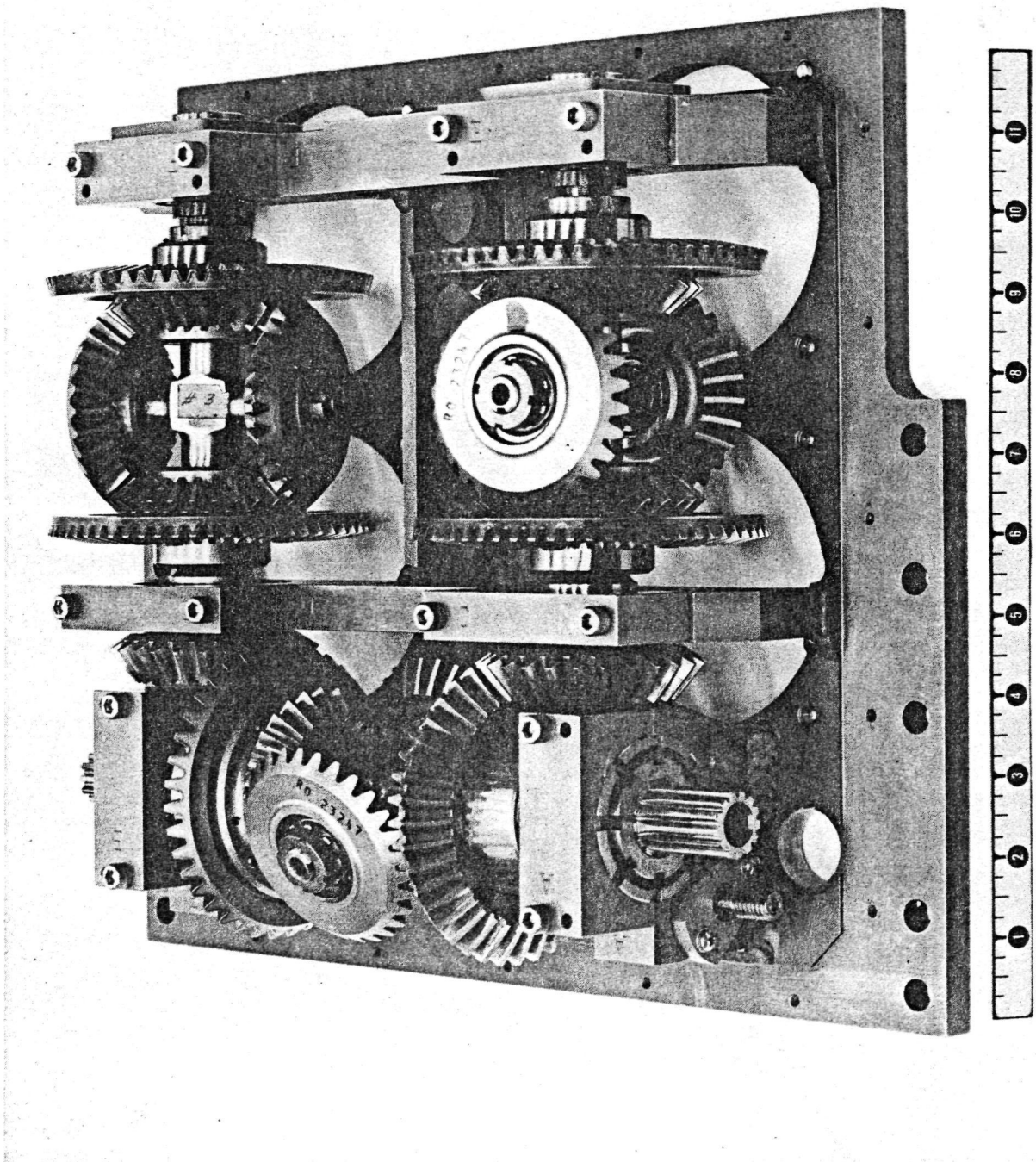

Figure 4-11. Differential Gearbox

The gearbox housing is made of aluminum, welded and machined after welding. Oil splash type lubrication is provided for the gears.

The major gearbox power train performance characteristics are summarized below.

Maximum input speed	9000 r/min
Average input speed	2250 r/min
Maximum input torque	120 in. lb
Maximum output torque	2700 in. lb
Maximum input power per motor	17 hp
Average input power per motor	5 hp
Maximum output speed	800 r/min
Gear ratio (two motors operating)	11.25:1

4.3 MOTOR ASSEMBLY

Figure 4-7 showed the four motors mounted on the differential gearbox. The rotor position sensor is located at the pinion end of the motor, and the brake and tachometer assembly is at the opposite end. The rotor is coupled to the brake disc assembly and to the tachometer which provides velocity feedback in the actuator system.

4.3.1 BRAKE

The brake consists of both a permanent magnet and an electromagnet. If the electromagnet is deenergized, the permanent magnet pulls the brake disc into contact with the stationary brake shoe, thus stopping the rotor. To release the brake, the electromagnet is energized, thus cancelling the field of the permanent magnet. A small spring pushes the brake disc away from the brake shoe to allow free rotation.

4.3.2 TACHOMETER

The tachometer is directly coupled to the motor shaft. It has a highly linear speed/voltage characteristic, operates bi-directionally, and is designed for long operating life. Important specifications for the tachometer are listed in Table 4-1.

Output voltage gradient	7.0 V/1000 r/min
Output impedance, maximum	350 ohms
Output linearity, 100 to 6000 r/min	0.1%
Ripple voltage, maximum RMS	3%
Bi-directional output voltage error	0.25%
Maximum speed	12,000 r/min
Friction torque, maximum	0.25 oz-in.
Armature inertia, maximum	6.5 gm-cm^2
Weight, maximum	3.0 oz
Mechanical natural frequency, minimum	1800 Hz
Life expectancy at 3600 r/min	10,000 hr

Table 4-1. Tachometer Specifications

4.3.3 ROTOR

Figure 4-12 shows the rotor with the samarium cobalt magnets attached, and Figure 4-13 shows the rotor with end discs in place. The end discs reduce windage losses and provide material which can be removed during dynamic balancing.

4.3.4 STATOR

Figure 4-14 shows the stator before winding. The stator winding partially fills the slots, and the rotor is separated from the stator by an airgap and a sleeve. Coolant enters one end of the stator assembly, flows through the partially filled slots, and exits through the outlet at the far end. The Thermal Control System for the motor is described in paragraph 4.5.

4.3.5 PHYSICAL CHARACTERISTICS

Pertinent physical characteristics and efficiency of the motor are listed in Table 4-2.

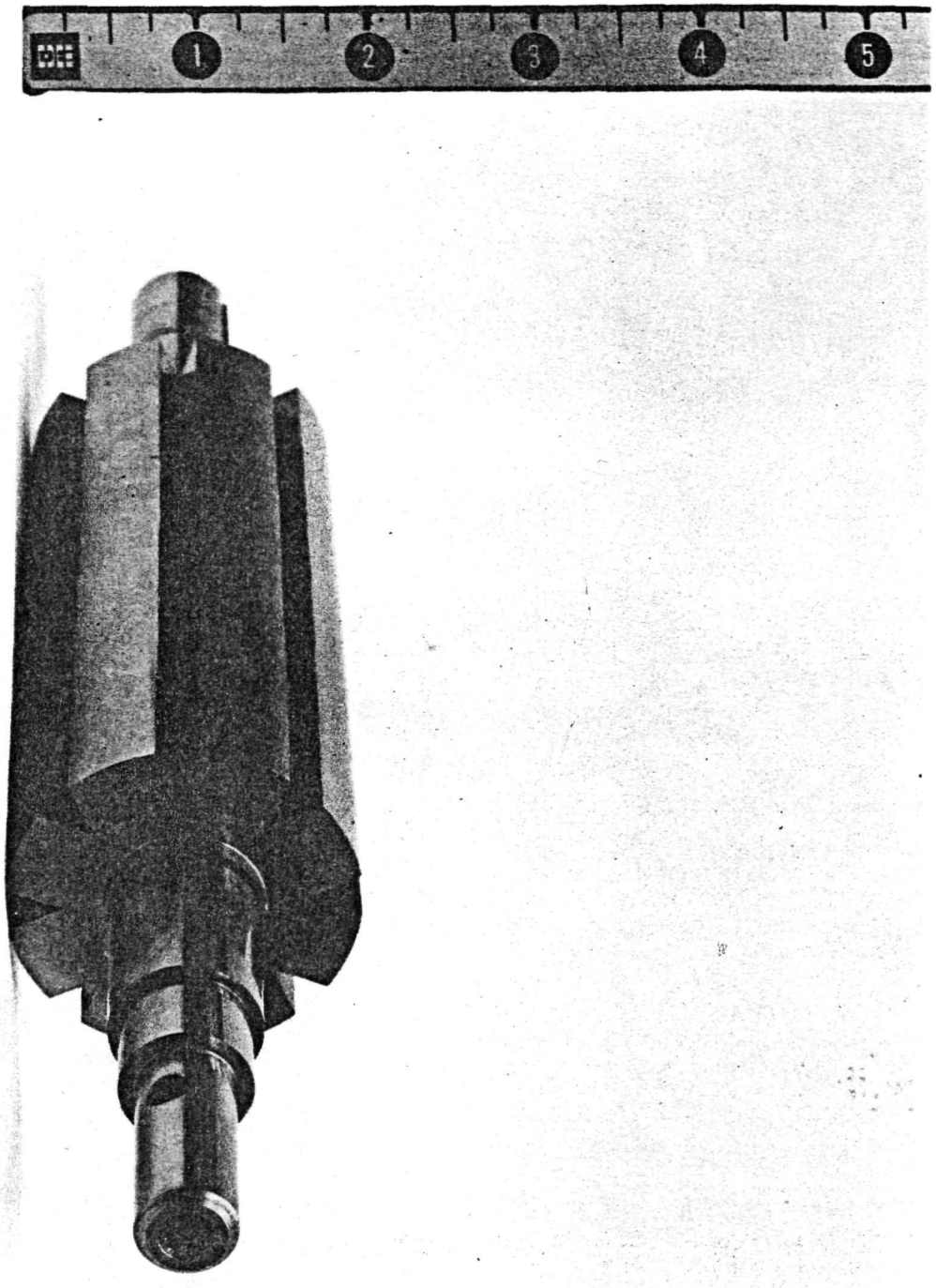

Figure 4-12. Rotor With Samarium Cobalt Magnets

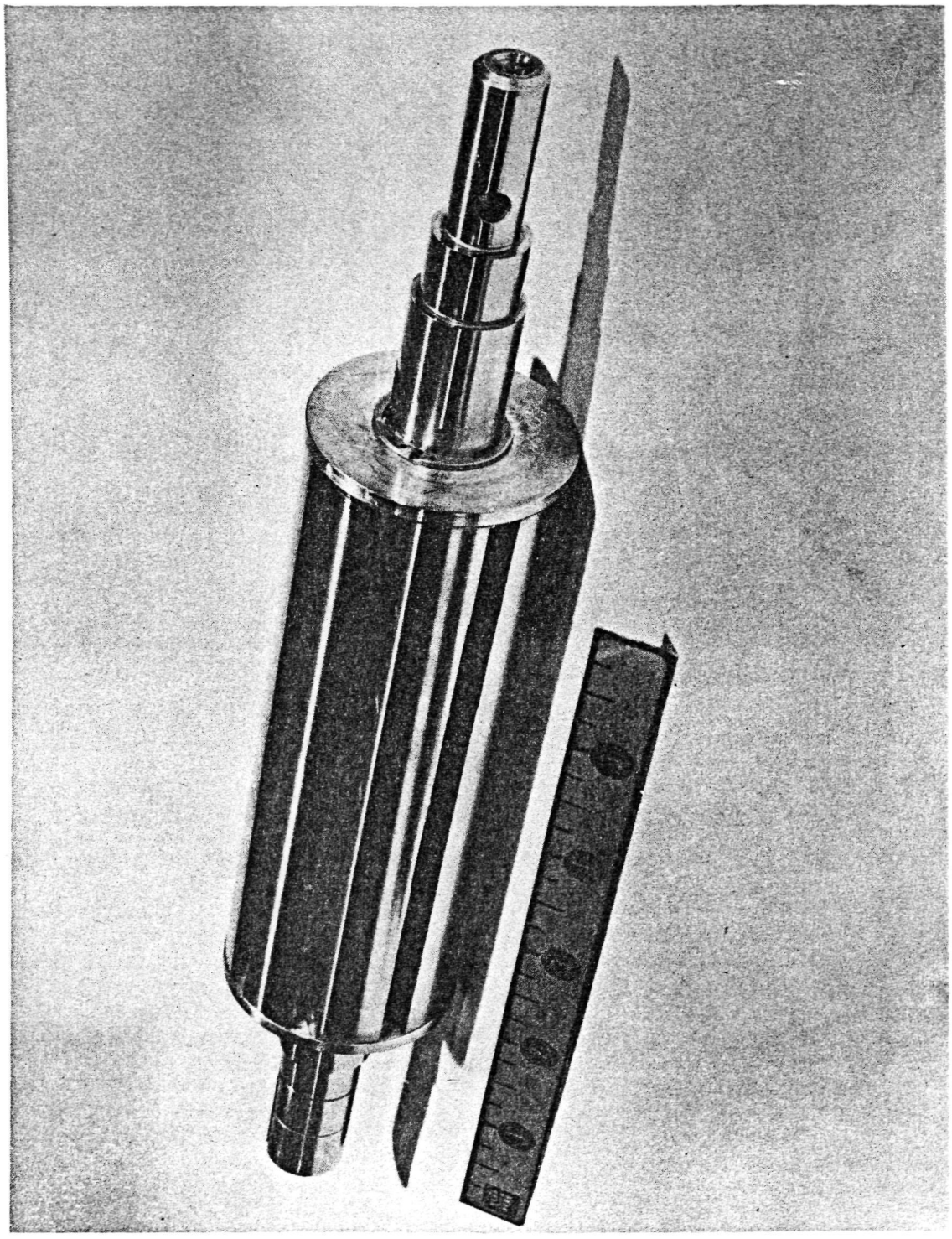

Figure 4-13. Rotor With End Discs Installed

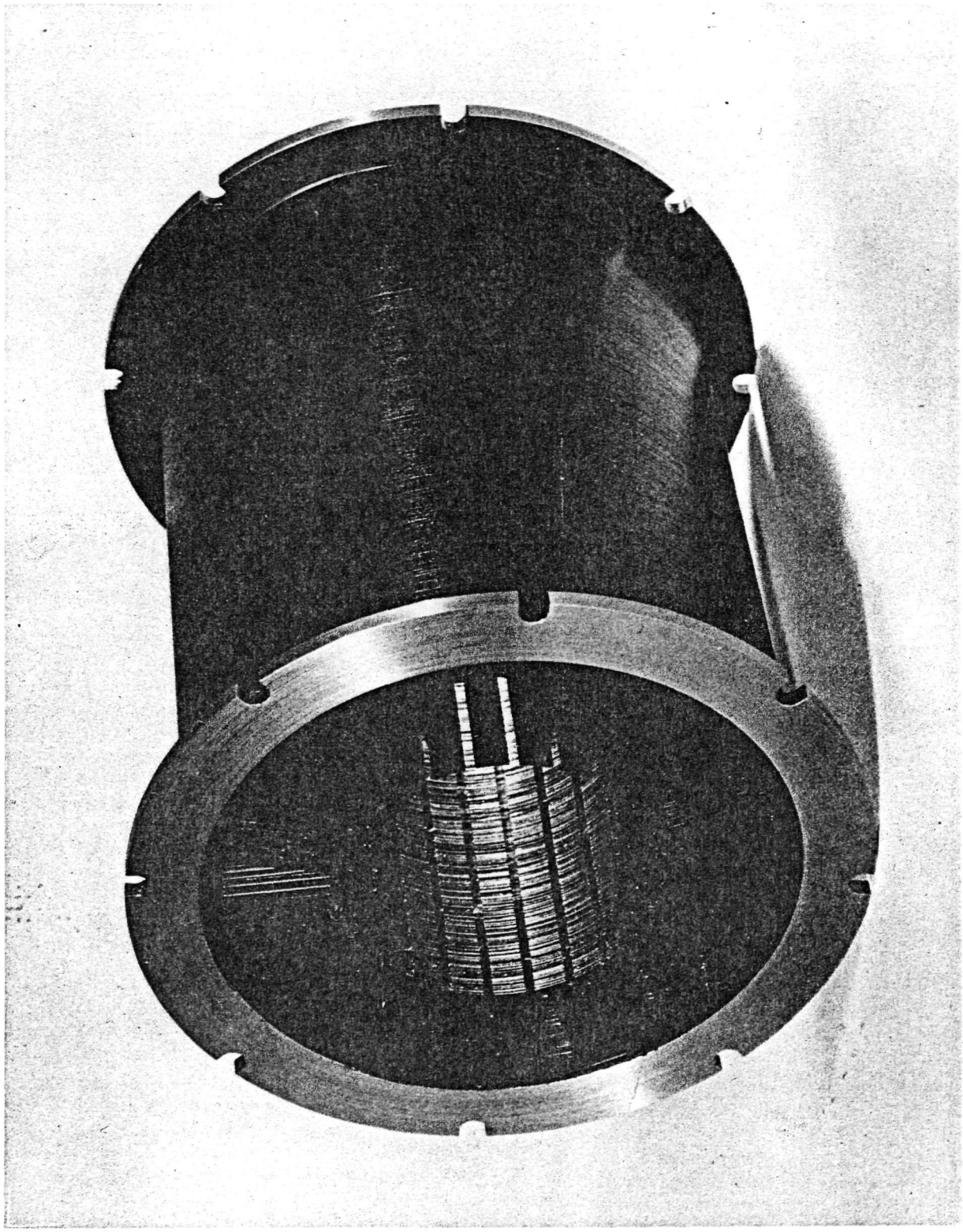

Figure 4-14. Stator

SIZE	PROPOSED	ACTUAL
LENGTH OVER BRAKE	11.85 inches	11.25 inches
DIAMETER OF MOTOR FRAME	3.75 inches	3.75 inches
WEIGHT	**DESIGN GOAL**	**ACTUAL**
MOTOR, RPS AND CABLE	17.0 lb	17.16 lb
BRAKE, TACH, COUPLING	5.0 lb	2.7 lb
EFFICIENCY	> 95%	> 92.6%

Table 4-2. Motor Physical Characteristics and Efficiency

4.4 CONTROL ELECTRONICS

4.4.1 PHYSICAL ARRANGEMENT

The electronics for the four-channel EM actuator are housed in a conventional equipment rack (Figure 4-15). The power control electronics are located at the top. The volume immediately below the power control panel is presently empty, but it is anticipated that the redundancy management electronics would eventually be housed here. Below this area are two drawers of control electronics, each of which contains two channels of low-level electronic equipment. The main power electronics assembly is located immediately below the control drawers. The bottom part of the rack contains the power contactors, 28 Vdc power supply for the system, and the brake control electronics chassis.

Figure 4-16 is a close-up view of the power control panel and the two low-level electronics drawers. The power control panel provides the necessary sequencing switches to turn power on or off in the system, displays high voltage on-off and cooling system status, and contains the battery voltage and current meters. The control panels on the front of the

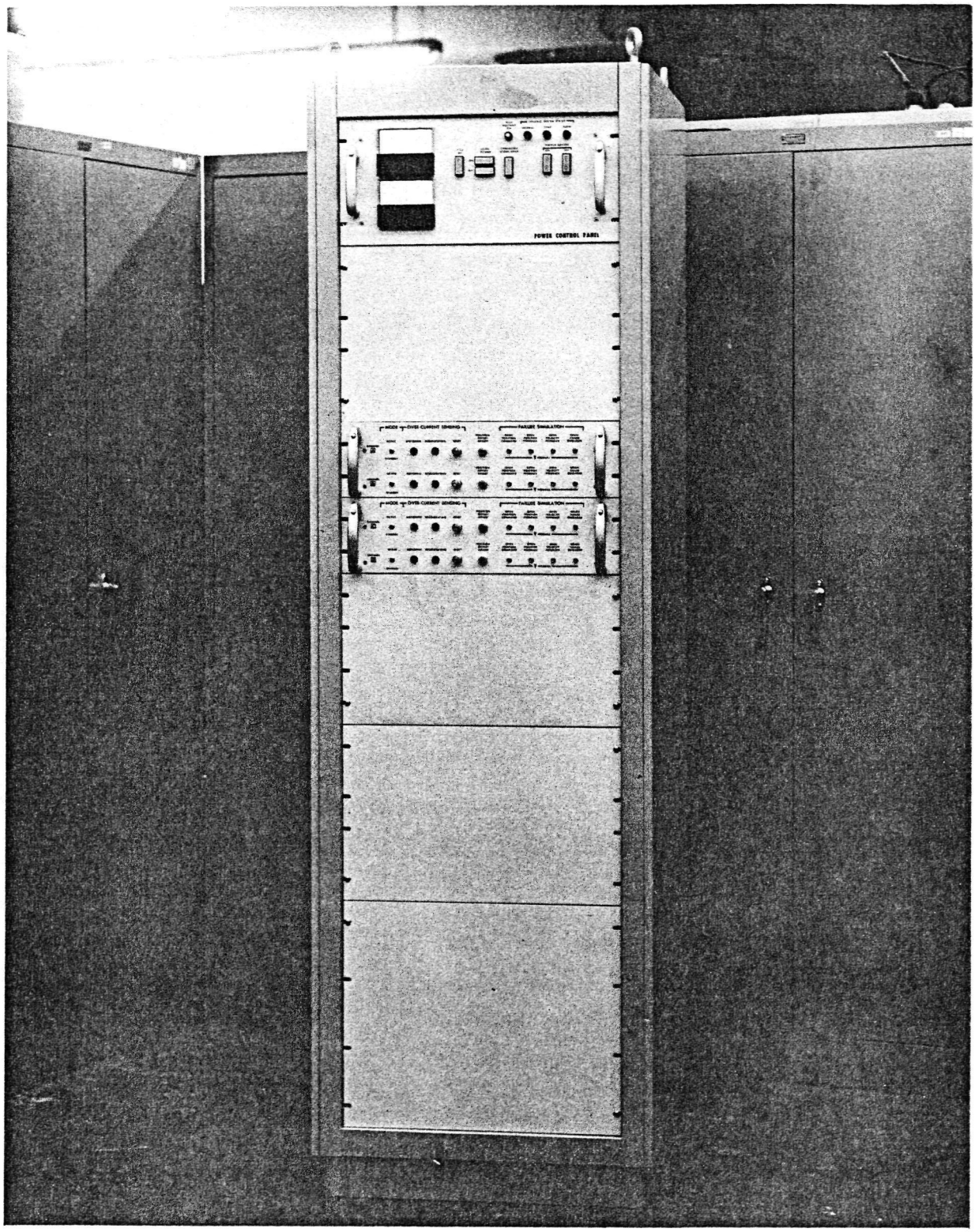

Figure 4-15. Electronics Rack

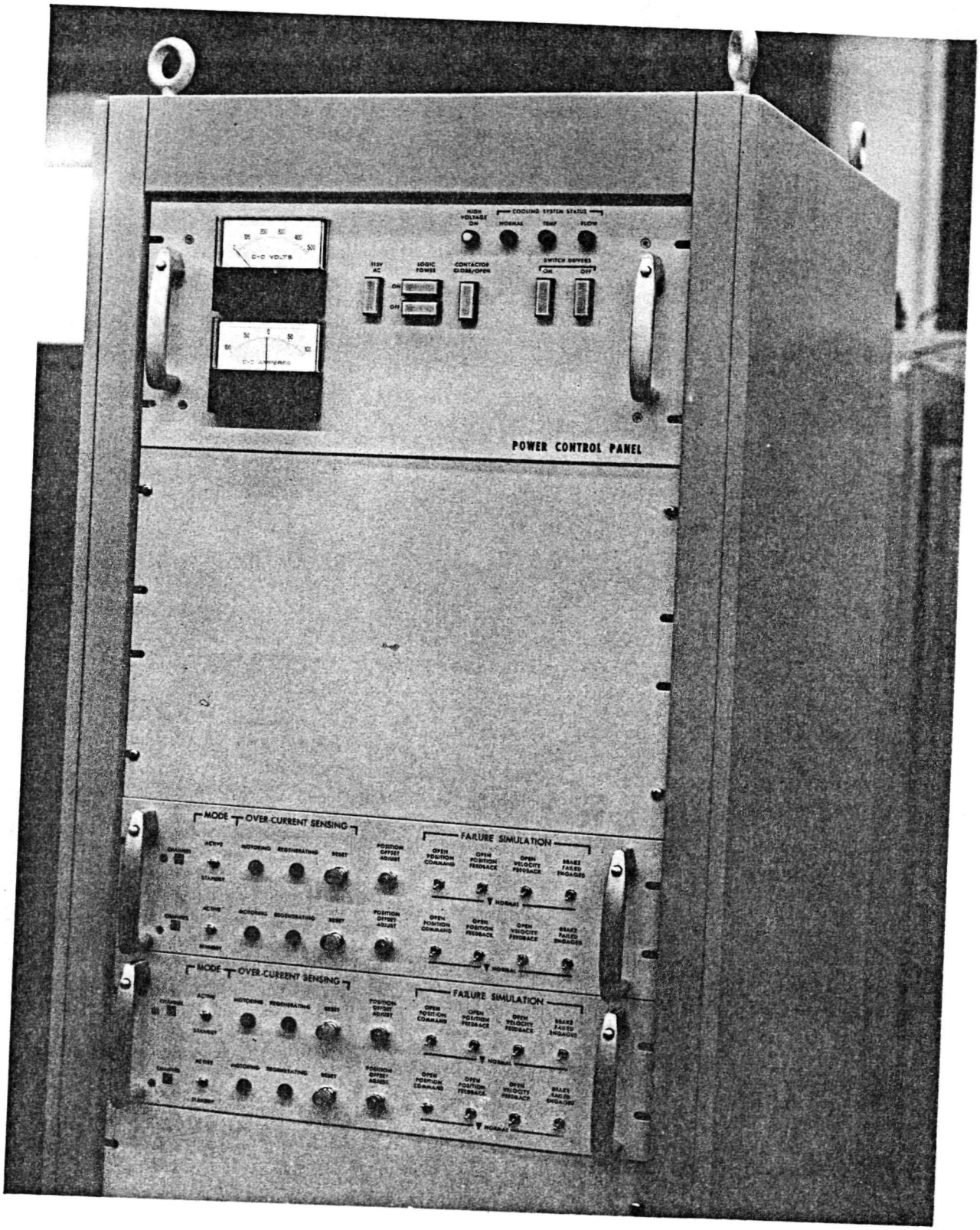

Figure 4-16. Power Control and Low-Level Electronics Panels

low-level electronics drawers allow each channel to be placed in either an active or standby mode, via a two-position toggle switch. Over-current sensing indicators are provided for each channel that remain illuminated after an over-current condition is detected until reset by means of a momentary push button. A position offset adjustment is also available on the panel (a locking, screwdriver-adjustable potentiometer is used for this purpose). Failure simulation switches are provided for future redundancy management studies, but they are not presently wired into the control circuits.

4.4.2 LOW-LEVEL ELECTRONICS

The low-level electronics (Figure 4-17) consist primarily of dual-in-line packages (DIPs). Where necessary, discrete components are mounted on special adapters and plugged into the major assembly. Connections to other parts of the electronics rack are made through connectors on the rear of the drawer. The digital logic is CMOS which operates from a 12 V supply. The low-level analog circuitry operates from ±12 V. Figure 4-18 shows one of the circuitboards in the upright position. The connections are wire wrapped to allow circuit changes to be made easily, and are very convenient for brassboard development. In addition, the wire wrap posts allow ready access to any of the circuit nodes; this is very valuable during system checkout and testing.

4.4.3 POWER ELECTRONICS

The power source used for the power electronics is the same as that described for the Delco Breadboard System (ref. paragraph 4.1.1). Figure 4-19 shows the power electronics drawer. The four power circuits are mounted on two heatsinks. Each of the four power converters uses four power switch assemblies (dual integrated power switches, Texas Instruments, Inc.). Also mounted on the drawer are the inductor, filter capacitors, and the current shunt used to measure the current being sent through the power converter. Fuses for the three motor leads are shown on the upper right hand corner of the heatsink assembly. Liquid cooling lines are brought in at the upper left hand corner of the assembly and provide coolant flow through the heatsink structure. The power supplies for the power switches are mounted in the channel shown at the bottom of Figure 4-19. These isolated supplies provide necessary logic power for the power switches.

The dual integrated power switches, rated at 60 A, 390 V, are designed for use in precision power conversion equipment. Typical switching time at rated current is 0.5 μs.

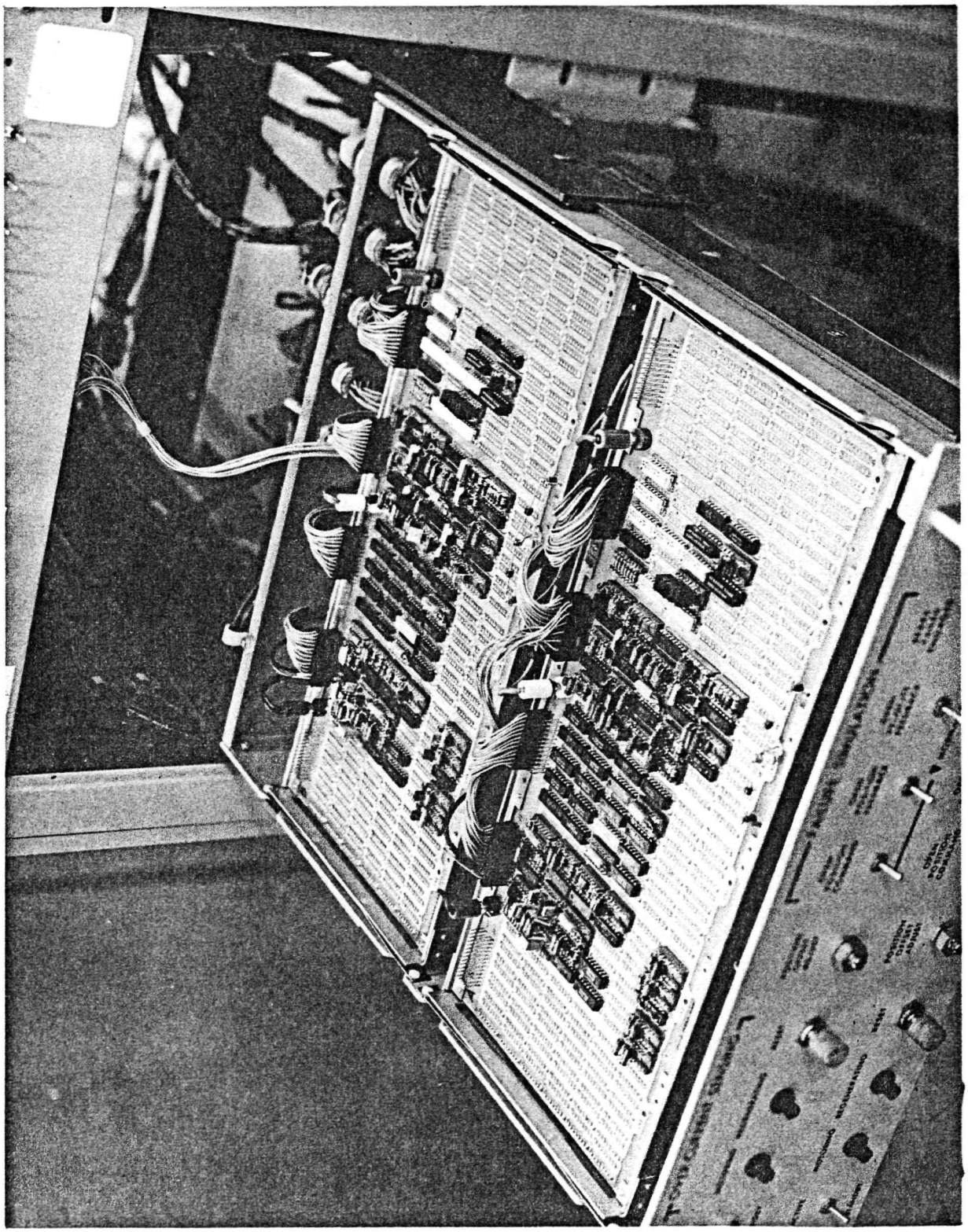

Figure 4-17. Low-Level Electronics (Extended Position)

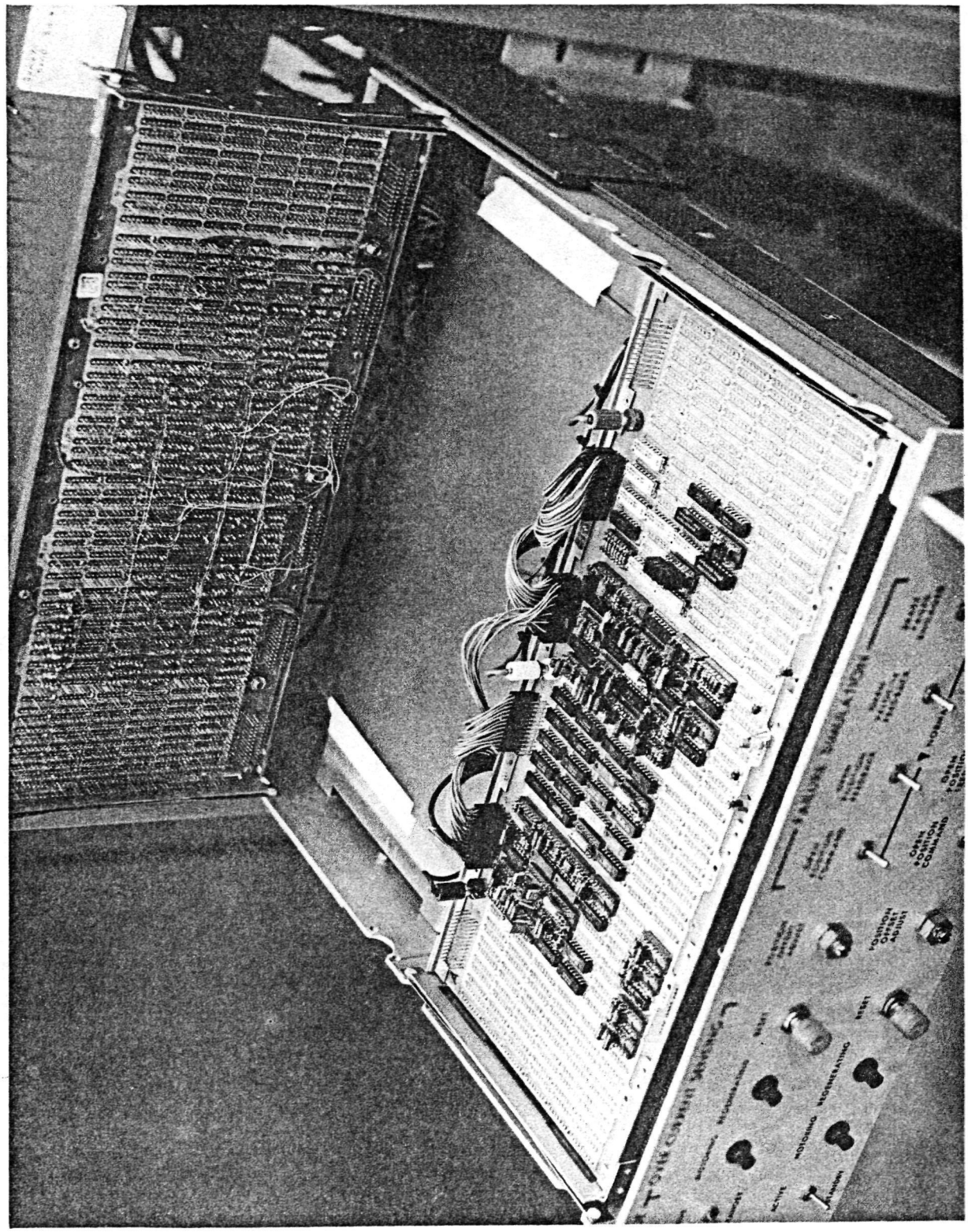

Figure 4-18. Low-Level Electronics

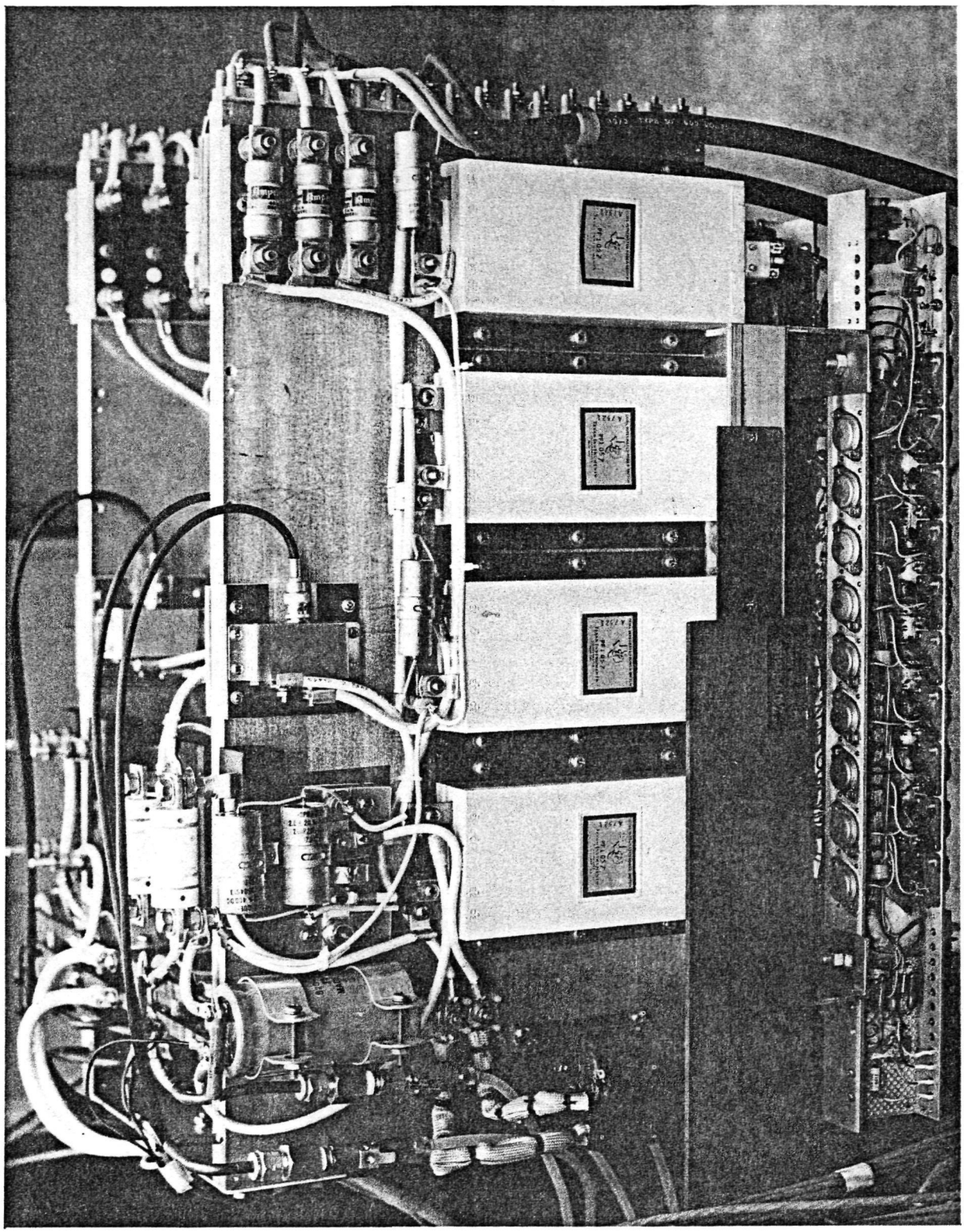

Figure 4-19. Power Electronics Assembly

Each dual switch contains two identical circuits which may be connected together for a single push-pull output or operated as two independent switches. It features optically coupled isolation between input circuitry and power system. Internal circuitry turns off each switch within approximately 2 μs if its load is short-circuited. Approximately 2.5 ms after turnoff caused by a short circuit, the switch becomes operational again. Should the short circuit still exist, the switch will turn off again and recycle at a frequency of approximately 400 Hz until the short circuit condition is removed. Protection is also provided against overheating; the signal for this condition is fed into a Schmitt trigger which, because of its hysteresis, assures that the temperature recovers by a safe margin before operation resumes.

4.5 THERMAL CONTROL SYSTEM

A thermal control system was designed and built to provide liquid cooling for the electric motors. The coolant is introduced into one end of the motor stator assembly. The stator has a nonmetallic sleeve in the airgap which provides a path for the cooling fluid through the stator slots. The coolant flows through the stator axially, and exits at the opposite end. Rotor cooling is not required, since the permanent magnet rotor has no power dissipation.

The thermal control system is designed as a self-contained unit housed in a reduced height console. It consists of an oil-to-air heat exchanger, circulating pump, reservoir with associated valves, filters, etc., and a temperature monitoring panel (Figure 4-20).

Each of the four motors is supplied cooling fluid by a central pump through four parallel loops. The pump supplies a constant pressure head to each motor, which has matched pressure drops, so that a constant flow is obtained through each motor. A pressure relief valve is incorporated to protect the motors from overpressure.

The cooling fluid selected is Coolanol 40 with a flash point of 370° F, and a boiling point of 700° F at 1 atm. The cooling fluid temperature can be controlled by varying the amount of air allowed to flow through the heat exchanger by means of louvers or on/off blower motor control. An over-temperature switch in the reservoir turns off the motors when fluid temperature approaches the flash point. A pressure sensor in the motor inlet line monitors the presence of coolant flow. Temperature sensors (thermocouples) at the input

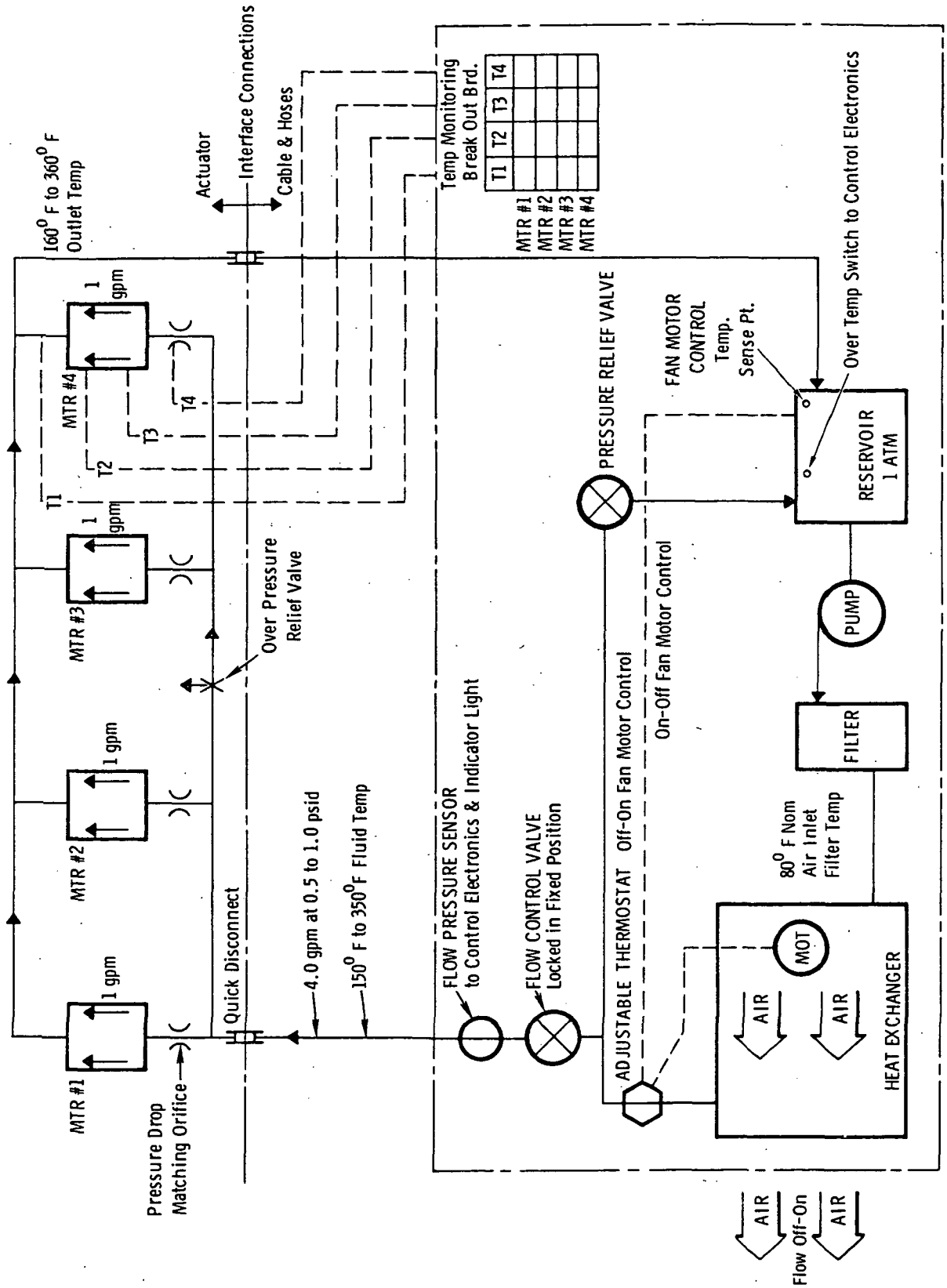

Figure 4-20. Functional Diagram - Thermal Control System

and output points to the motors and a coolant flow meter allow the determination of motor heat rejection through the cooling fluid. A terminal board is mounted on the front panel of the cooling assembly where coolant, motor, brake, etc., temperatures can be monitored.

SECTION V
RECOMMENDATIONS FOR FURTHER EFFORT

5.1 GENERAL

As a short range effort, the program should complete those tasks necessary to demonstrate the feasibility of the EM actuator concept and prepare for the design of prototype hardware. As a longer range effort, a prototype should be designed to satisfy the requirements of a specific application, and it should be built and tested to those requirements. The following discussion describes in more detail some of the near-term activities that should be undertaken.

5.2 LOAD STAND MODIFICATIONS

The gear reducer housing on the left end of the load stand moves during load motion. The housing should be more adequately secured before further tests are conducted.

Each clevis arm is keyed to the rotating member, allowing significant relative motion in this mechanism. A more rigid connection should be made (such as pinning these two members together). Since drawings are not available, it will be necessary to disassemble this portion of the load stand to determine the best way to resolve this problem.

5.3 DEVELOPMENT OF SYSTEM MATH MODELS

To obtain a deeper understanding of system characteristics and to allow the effects of design improvements to be predicted accurately, detailed math models of the system are needed. Subsystem modeling should include all major blocks such as the current source, inverter, motor, gearbox, tachometer (and its coupling), position transducer and control electronics. System models are needed to understand transient conditions, linearized frequency response characteristics and all major nonlinear effects such as backlash, torque limiting, and velocity limiting.

5.4 TESTING AND TEST INSTRUMENTATION

To provide needed test data, additional test instrumentation should be installed. Major needs include torque transducers to measure gearbox output torque, position transducers to measure load deflection, voltage and current instrumentation to allow accurate power measurements, and additional temperature transducers for thermal testing.

Efforts will be required to plan the tests, select instrumentation, and install and calibrate the selected transducers.

It is anticipated that data acquisition will consist of direct readout of test voltages, currents, temperatures, etc., under steady-state operating conditions, and the use of oscilloscopes or strip chart recorders to record transient data. Servo analyzers will be used for frequency response measurements.

5.5 CONFIRMATION OF MATH MODELS

A major purpose of the testing effort will be the acquisition of data to confirm the system math models. Where discrepancies are found, the test data and analytical models will be reviewed and necessary changes to the models will be developed.

5.6 OPTIMIZATION OF SYSTEM GAINS AND COMPENSATION METHODS

As a result of the analytical and test efforts, the system gains and compensation methods will be optimized to achieve the required system performance. Such measures as step response, sinusoidal response, efficiency, threshold and hysteresis will be used in this optimization process.

5.7 REDUNDANCY MANAGEMENT STUDIES

Redundancy management studies should be conducted to evaluate such basic system concepts as:

- Two active, two standby channels
- Three active, one standby channel
- Four active channels, reduced performance after failure

Basic concepts for failure detection must be established, with performance monitoring concepts being defined and methods formulated for minimizing the possibility of faults caused by the monitoring techniques.

The feasibility of providing effective redundancy management must be established, and basic algorithms for actions to be taken following fault detection must be developed. In addition, the transient effects which result from major faults must be evaluated to assure that they do not result in a major disturbance.

5.8 POWER ELECTRONICS IMPROVEMENTS

The operating modes of all power components should be evaluated carefully to establish their design margins. Where inadequacies are found, recommendations should be made regarding methods to be used to provide safe operating regimes for all power components. Critical analyses and/or experiments should be conducted to verify that the proposed approach is suitable.

5.9 MOTOR IMPROVEMENTS

Critical design considerations for the motor (such as shock, vibration, temperature, and operating duty cycle) should be established, and the motor design examined to determine any required changes to assure adequate design margins. Where necessary, critical tests and analyses should be conducted to confirm that a motor can be built to meet all design requirements.

APPENDIX A
SERVO ANALYSIS

SIMPLIFIED LINEAR ANALYSIS

A simplified, linearized block diagram of the EM actuator is given in Figure A-1. Although this diagram ignores all system lags other than that associated with the motor/current source, it is very useful for analyzing the effects of major system gains, inertias, and gear ratios. In the diagram, δ_o is the output motion of the load (in degrees), ω_o is the angular velocity of the load (degrees/second), N_M is the motor angular velocity (in r/min), T_M is the motor torque (in inch-lb), I_A is the motor armature current (amperes), and I_c is the commanded armature current (amperes). The commanded load deflection, δ_c (in degrees), is compared with the actual load deflection, δ_o, and the error signal is amplified (with gain K_E) to provide control signal E. The velocity feedback signal, V, is subtracted from E to form the current command, I_c. For this analysis, the current source and motor effects are represented by a single first-order lag with time constant τ (seconds). The motor torque coefficient, K_T (in-lb/A), converts the armature current to a torque which is applied to the inertia of the system, J (in-lb-s^2), reflected to the motor shaft. The integrated acceleration (with appropriate scaling) results in a motor r/min, N_M. The gear ratio, a, (and proper scale factor) converts the motor angular velocity to load angular velocity. This is integrated to obtain the output (load) deflection, δ_o.

For convenience, let

$$K_1 = \frac{180K_T}{\pi J\, a} \qquad \text{(A-1)}$$

The system block diagram can then be simplified to that shown in Figure A-2.

INNER LOOP TRANSFER FUNCTION

From an analysis of the simplified system diagram, the inner loop transfer function is found to be:

$$\frac{\omega_o}{E} = \frac{\frac{K_1}{\tau}}{s^2 + \frac{1}{\tau}s + \frac{K_1 K_v}{\tau}} \qquad \text{(A-2)}$$

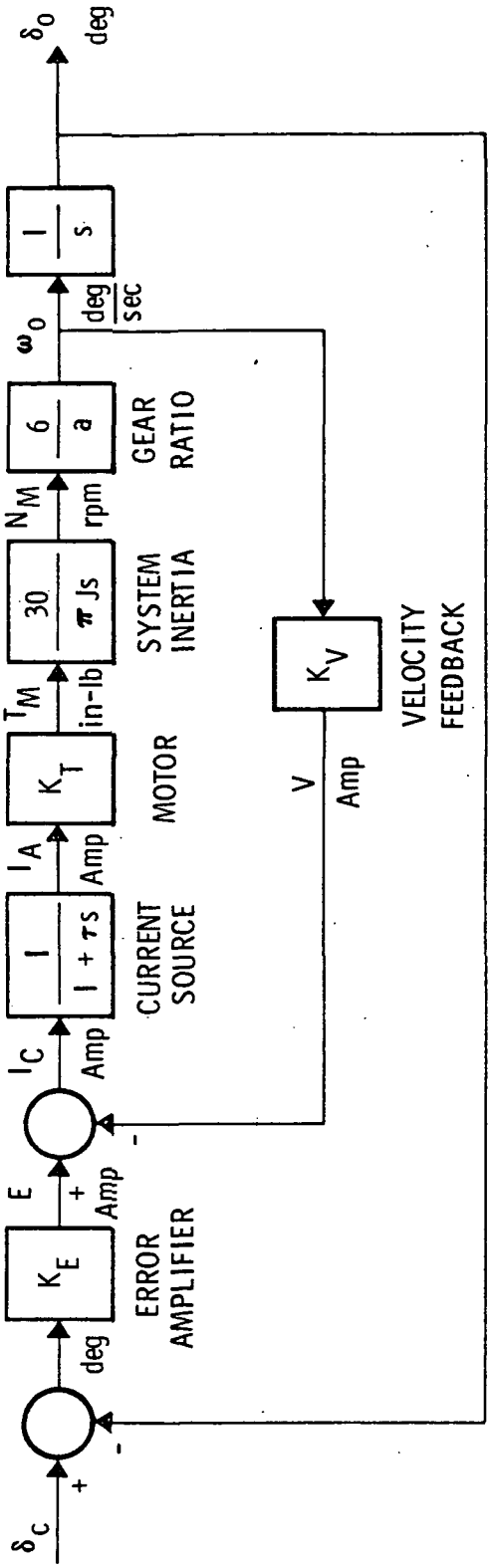

Figure A-1. EM Actuator Block Diagram

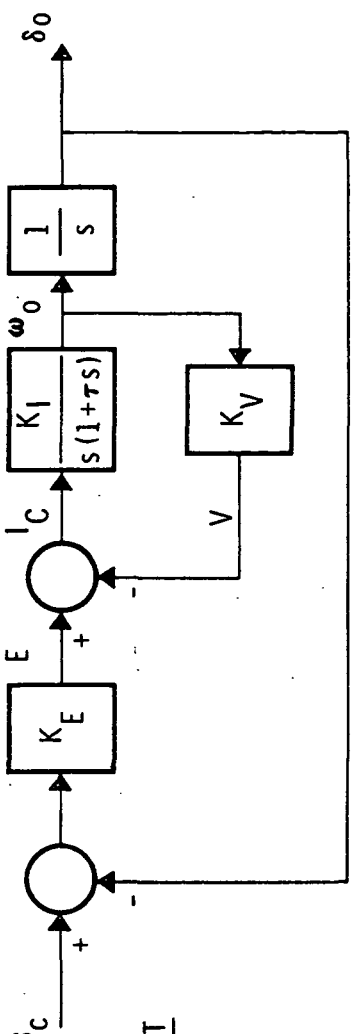

Figure A-2. EM Actuator Simplified Block Diagram

K_E Amp/deg
τ sec
K_T in-lb / Amp
J in-lb-sec^2
a dimensionless
K_V Amp / deg / sec

$$K_I = \frac{180\ K_T}{\pi\ Ja}$$

$$= \frac{\frac{1}{K_v}}{1 + \frac{1}{K_1 K_v} s + \frac{\tau s^2}{K_1 K_v}} \qquad \text{(A-3)}$$

A root locus plot for this loop is given in Figure A-3. For gains such that

$$K_1 K_v \leq \frac{1}{4\tau} \qquad \text{(A-4)}$$

it can be seen that the loop has two real poles. For higher gains, the loop has complex poles.

The natural frequency of the inner loop is

$$\omega_n = \sqrt{\frac{K_1 K_v}{\tau}} \quad \text{rad/s} \qquad \text{(A-5)}$$

and its damping ratio is

$$\zeta = \frac{1}{2\tau \omega_n} \qquad \text{(A-6)}$$

Figure A-4 shows asymptotic Bode plots for the inner loop. The natural frequency and damping ratio of the inner loop as a function of the loop gain, $K_1 K_v$, is shown in Table A-1.

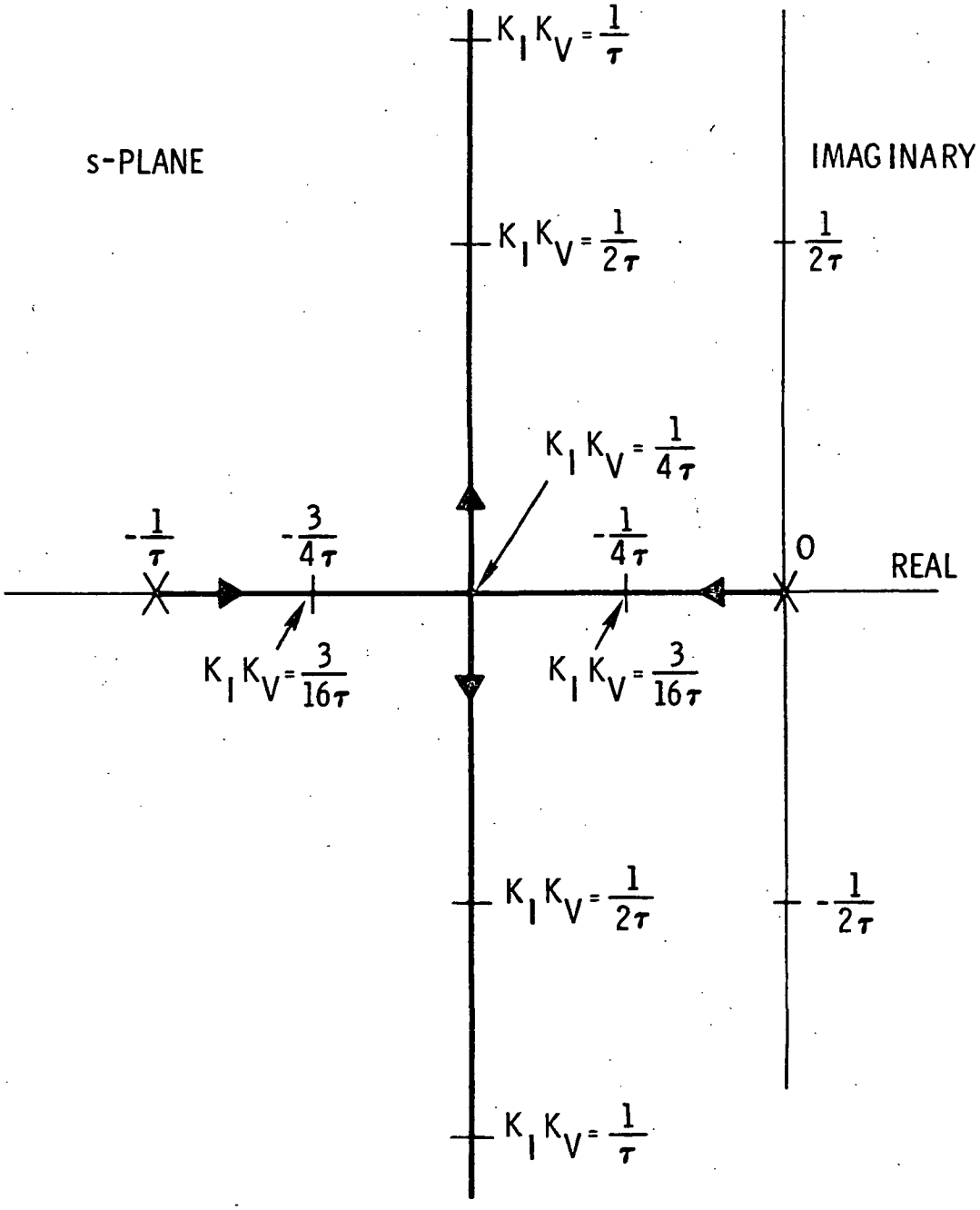

Figure A-3. Inner Loop – Root Locus

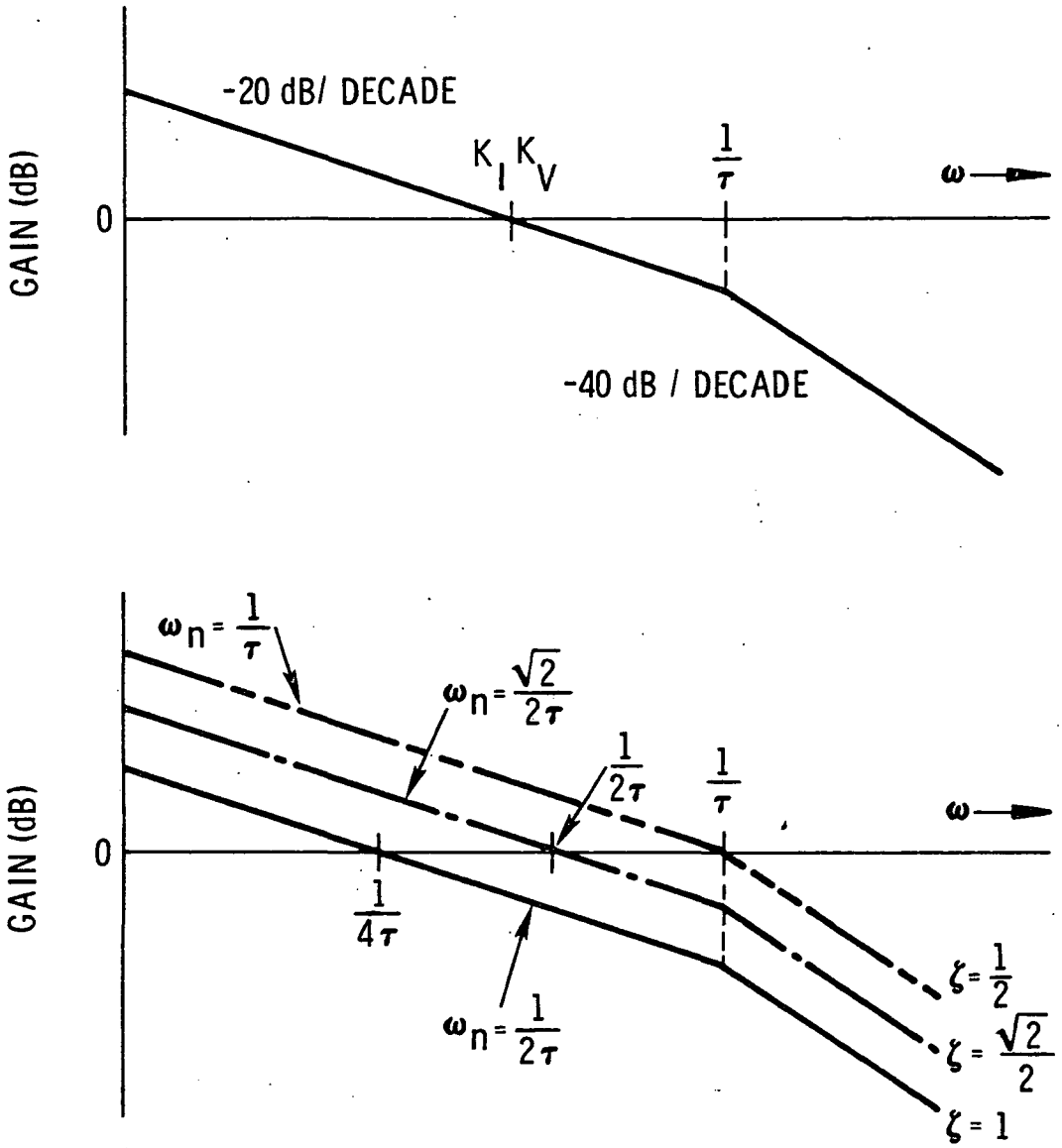

Figure A-4. Inner Loop Gain Bode Plots

$K_1 K_v$	ω_n	ζ
$\frac{1}{4\tau}$	$\frac{1}{2\tau}$	1
$\frac{1}{2\tau}$	$\frac{\sqrt{2}}{2}\frac{1}{\tau}$	$\frac{\sqrt{2}}{2} = 0.707$
$\frac{1}{\tau}$	$\frac{1}{\tau}$	$\frac{1}{2} = 0.5$
$\frac{2}{\tau}$	$\frac{\sqrt{2}}{\tau}$	$\frac{1}{2\sqrt{2}} = 0.354$
$\frac{4}{\tau}$	$\frac{2}{\tau}$	$\frac{1}{4} = 0.250$
$\frac{16}{\tau}$	$\frac{4}{\tau}$	$\frac{1}{8} = 0.125$

Table A-1. Inner Loop Natural Frequency And Damping

OUTER LOOP TRANSFER FUNCTION

The closed-loop transfer function for the system shown in Figure A-2 is given by

$$\frac{\delta_o}{\delta_c} = \frac{1}{1 + \frac{K_v}{K_E}s + \frac{s^2}{K_1 K_E} + \frac{\tau s^3}{K_1 K_E}} \qquad \text{(A-7)}$$

$$= \frac{\frac{K_1 K_E}{\tau}}{s^3 + \frac{1}{\tau}s^2 + \frac{K_v K_1}{\tau}s + \frac{K_1 K_E}{\tau}} \qquad \text{(A-8)}$$

The Routh table for the characteristic equation of the system is

s^3	1	$\frac{K_v K_1}{\tau}$
s^2	$\frac{1}{\tau}$	$\frac{K_1 K_E}{\tau}$
s^1	$\left(\frac{K_1 K_v}{\tau} - K_1 K_E\right)$	
s^0	$\frac{K_1 K_E}{\tau}$	

The system will be stable if all elements in the left-hand column of the array are positive. This requires that τ, K_1 and K_E all be positive, and that

$$K_E < \frac{K_v}{\tau} \tag{A-9}$$

When $K_E = \frac{K_v}{\tau}$, the characteristic equation of the system becomes

$$s^3 + \frac{1}{\tau} s^2 + \frac{K_v K_1}{\tau} s + \frac{K_v K_1}{\tau^2} = 0 \tag{A-10}$$

For this condition, the roots are

$$s_1 = -\frac{1}{\tau} \tag{A-11}$$

and

$$s_2, s_3 = \pm j \sqrt{\frac{K_v K_1}{\tau}} \tag{A-12}$$

Root locus plots for the outer loop can have the two general characteristics shown in Figures A-5 and A-6. When the open-loop poles are all real (Figure A-5), the root locus for the system shows that the closed-loop poles will all be real when the loop gain is low. At higher gains, the two lower frequency poles merge and break away from the real axis forming complex pairs.

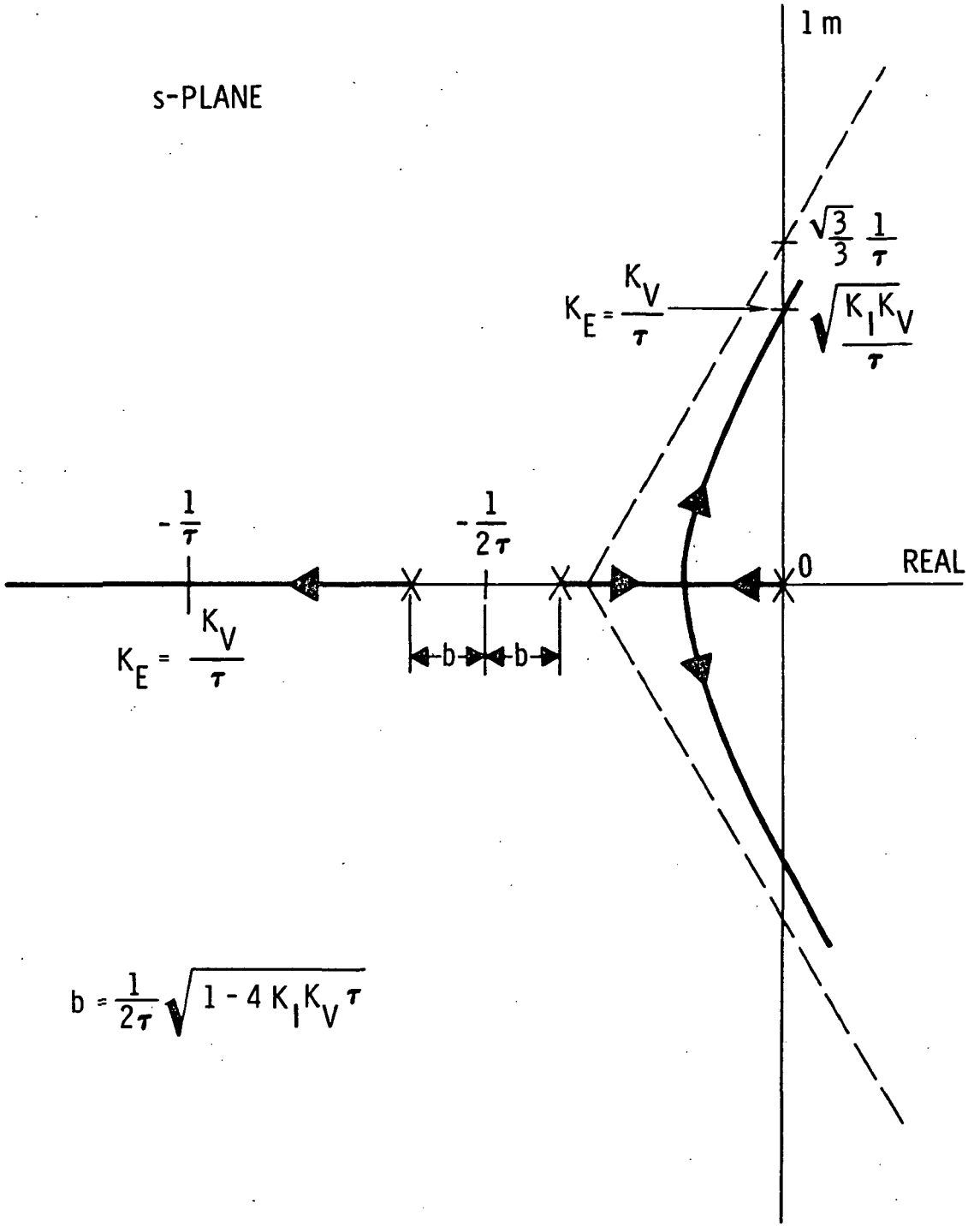

Figure A-5. Root Locus – Three Real Open-Loop Poles

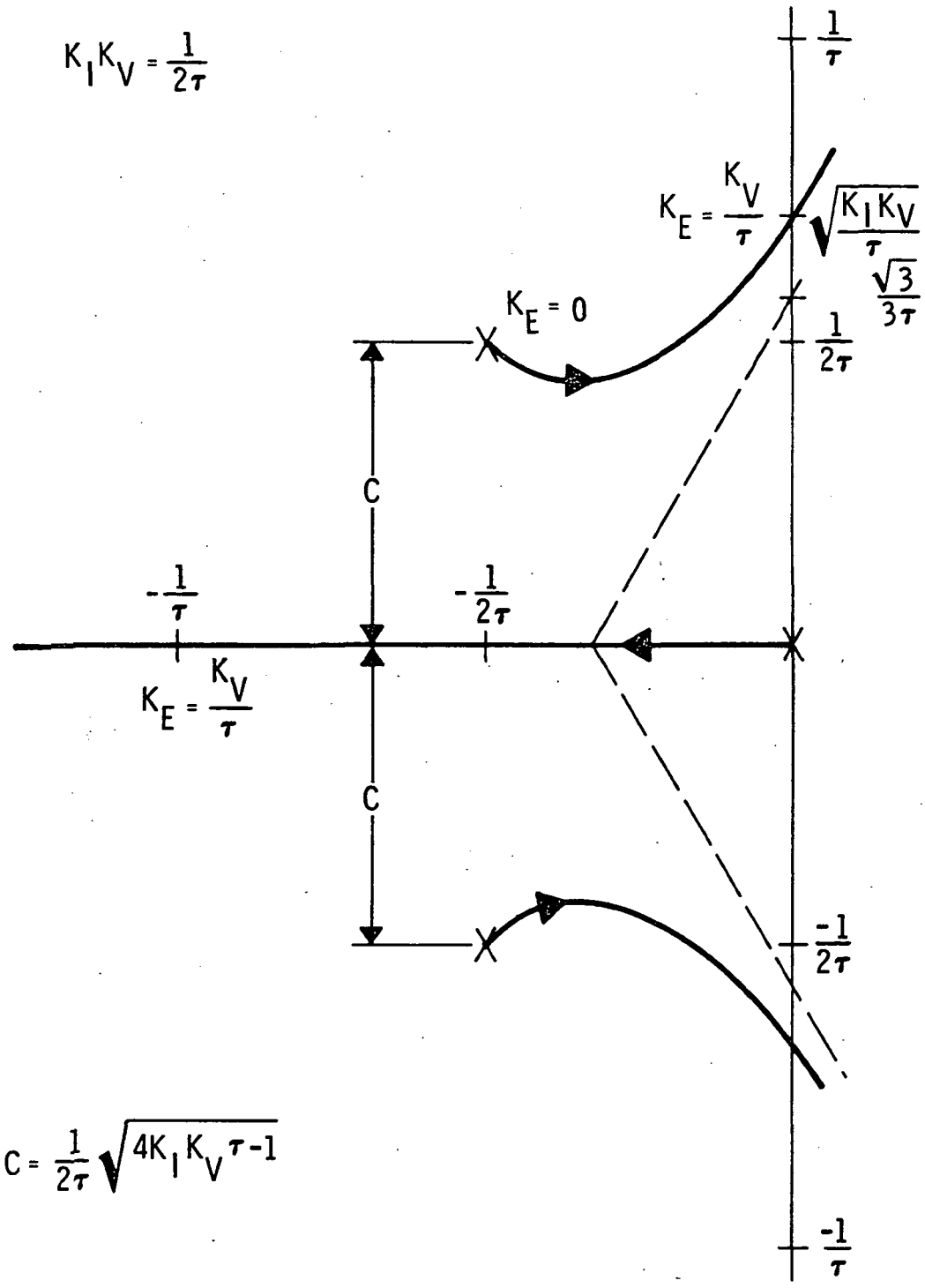

Figure A-6. Root Locus – One Real and Two Complex Open-Loop Poles

If the open-loop poles include a complex pair (Figure A-6), the closed loop will have one real pole and two complex conjugate poles. Typical asymptotic Bode plots for the two possible open-loop conditions are shown in Figure A-7.

As a special case which provides very important insights as to the effects of system parameters, consider the case where the system's dominant time constant, τ, is small enough to be neglected. For this case, the closed-loop transfer function of Eq. A-7 can be simplified to:

$$\frac{\delta_o}{\delta_c} = \frac{1}{1 + \frac{K_v}{K_E} s + \frac{s^2}{K_1 K_E}} \qquad \text{(A-13)}$$

For this case, the natural frequency of the actuator is:

$$\omega_N = \sqrt{K_1 K_E} = \sqrt{\frac{180 K_T K_E}{\pi J a}} \quad \text{rad/s} \qquad \text{(A-14)}$$

and the damping ratio is

$$\zeta = \frac{\omega_N}{2} \frac{K_v}{K_E} = \frac{K_v}{2} \sqrt{\frac{K_1}{K_E}} = \frac{K_v}{2} \sqrt{\frac{180 K_T}{\pi J a K_E}} \qquad \text{(A-15)}$$

These equations clearly indicate the effects of system gains, inertia, and gear ratio on the linear response characteristics of the system. Although this analysis is too oversimplified to provide a quantitative representation of the system's characteristics, it does represent the ideal situation which would be achieved if all system lags were negligible. More accurate analyses must include the effects of all dominant poles and zeroes, and must also take into consideration such nonlinear effects as torque limiting, velocity limiting, and gear backlash.

TORQUE AND VELOCITY LIMITING

STEP RESPONSE WITH TORQUE AND VELOCITY LIMITING

If the actuator were ideal, except for velocity and torque limiting, its behavior when responding to a step command would be as shown in Figure A-8 (assuming all loading effects other than the system's inertia are negligible). During the initial portion of the step

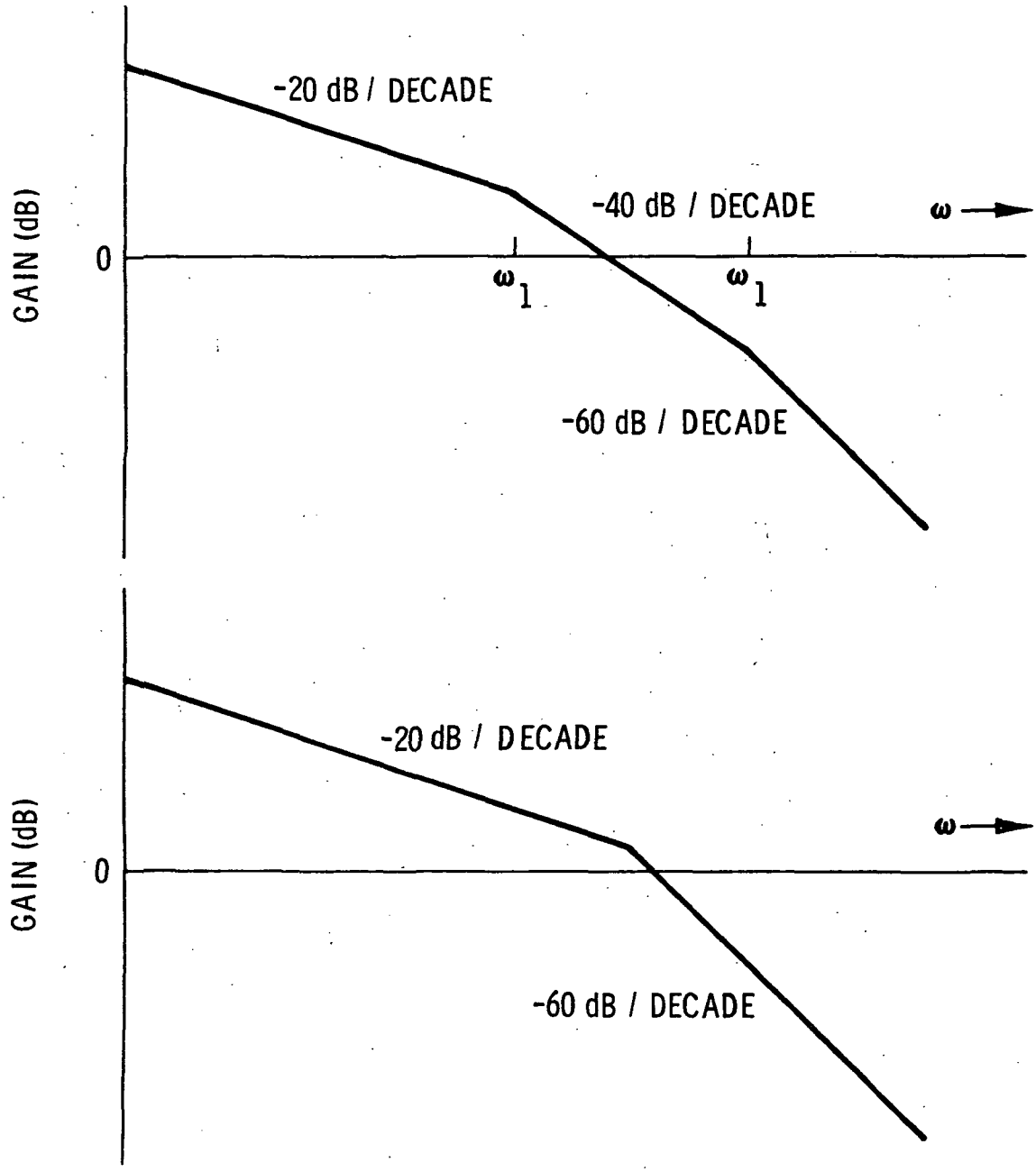

Figure A-7. Asymptotic Bode Plots

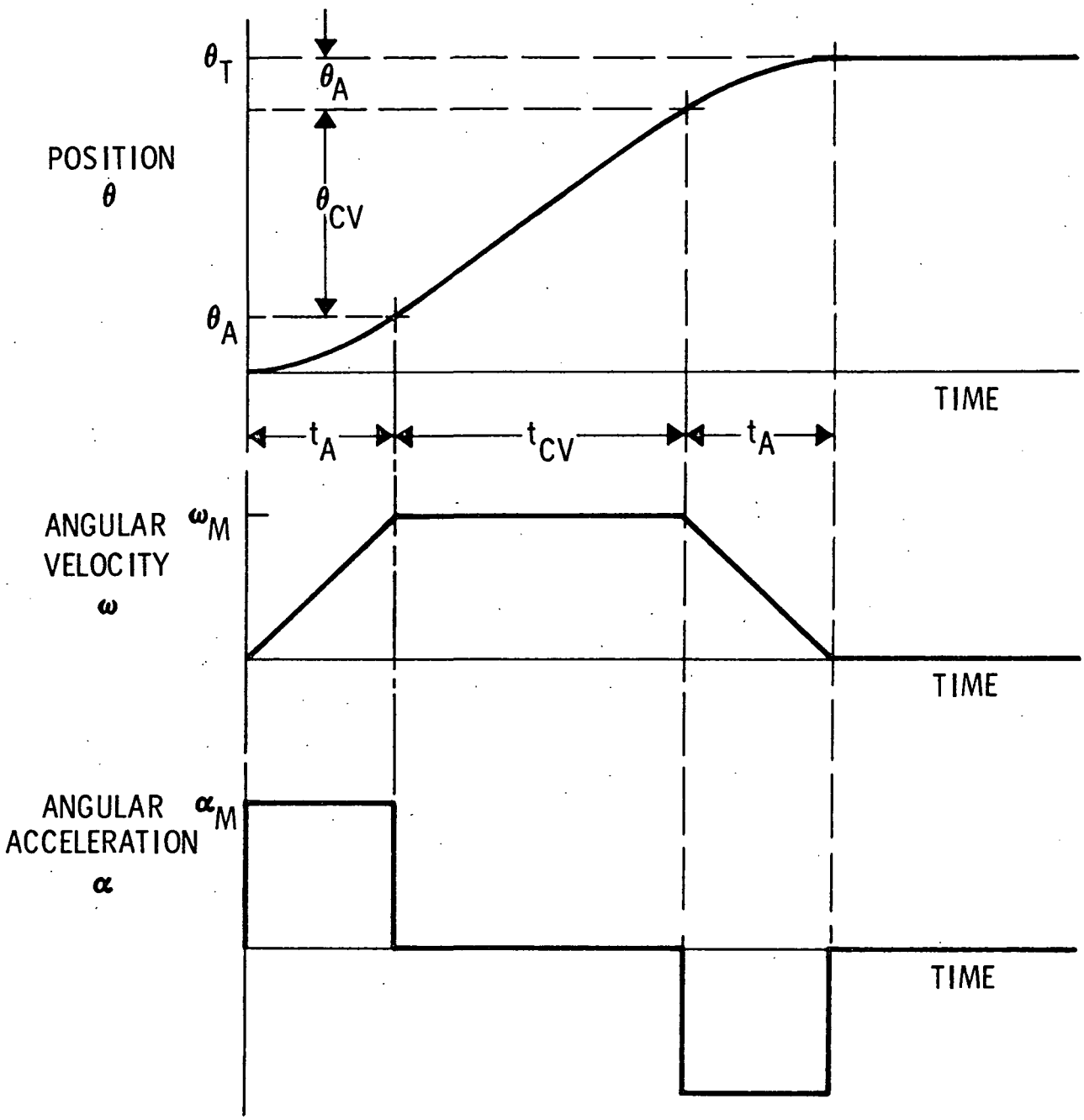

Figure A-8. Step Response of Idealized Actuator with Velocity and Acceleration Limiting

response, the motor would operate at full torque, thus achieving a constant acceleration. After the velocity limit is reached, the motion continues with constant velocity. As the load approaches the commanded position, full negative torque would be applied, decelerating the system inertia to its commanded position without overshoot. This idealized behavior can be analyzed using the following notation:

Symbol	Description, units
I_M	Maximum motor current, amperes
J	System inertia reflected to motor axis, in-lb-s^2
K_T	Motor torque coefficient, in-lb/A
N_M	Motor maximum speed, r/min
T_M	Maximum motor torque, in-lb
t_A	Time to accelerate to maximum velocity, seconds
α	Motor angular acceleration, rad/s^2
ω	Motor angular velocity, r/min
θ	Motor angular position, degrees
θ_A	Motor travel in accelerating to maximum velocity, degrees
θ_T	Total motor travel, degrees
δ_E	Load angular position, degrees
δ_{E_A}	Load angular motion required in accelerating to maximum velocity, degrees

The time required to accelerate the load to maximum velocity is given by

$$t_A = \frac{\pi}{30} \frac{N_M J}{K_T I_M} = \frac{\pi}{30} \frac{N_M J}{T_M} \quad \text{s} \qquad \text{(A-16)}$$

The angle traveled in reaching full speed is found to be:

$$\theta_A = \frac{\pi}{10} \frac{N_M^2 J}{T_M} \quad \text{deg} \qquad \text{(A-17)}$$

The time required to traverse a large angle (the case where velocity limiting occurs) is

$$t_T = \frac{\theta_T}{6N_M} + \frac{\pi}{30}\,\frac{N_M J}{T_M} \quad \text{s} \qquad \text{(A-18)}$$

The time required to travel through a small angle (without reaching velocity limiting) is

$$t_T = \sqrt{\frac{\pi\theta_T J}{180\,T_M}} \quad \text{s} \qquad \text{(A-19)}$$

where

$$\theta_T \le 2\theta_A \quad \text{deg} \qquad \text{(A-20)}$$

or

$$\theta_T \le \frac{\pi}{5}\,\frac{N_M^2 J}{T_M} \quad \text{deg} \qquad \text{(A-21)}$$

As a design example, if the maximum motor speed is 9000 r/min (corresponding to a load angular velocity of 20 deg/s), the step command is 2.0 degrees at the load, and

$J = 0.006$ in-lb-s^2 $\qquad$ $\theta_T = 5400$ deg

$T_M = 120$ in-lb $\qquad$ $N_M = 9000$ r/min

then

$$t_A = \frac{\pi}{30}\,\frac{(9000)(.006)}{120} = 0.0471 \quad \text{s}$$

$$\theta_A = \frac{\pi}{10}\,\frac{(9000^2)(.006)}{120} = 1272 \quad \text{deg}$$

$$\delta_{E_A} = 1272\left(\frac{20}{9000 \times 6}\right) = 0.471 \quad \text{deg}$$

$$t_T = \frac{5400}{6(9000)} + \frac{\pi}{30}\left(\frac{9000 \times .006}{120}\right) = 0.1471 \quad \text{s}$$

Thus, a step load command of 2.0 deg. is completed in 0.1471 s. The load reaches maximum velocity in 0.0471 s. During this time the load has traveled 0.471 deg (and the motor has rotated 1272 deg).

For the same design example conditions, velocity limiting would be reached for step angular commands (referred to the motor axis) greater than:

$$\theta_T = \frac{\pi}{5} \frac{(9000)^2(0.006)}{120} = 2545 \quad \text{deg}$$

which would correspond to a load deflection of

$$\delta_E = 2545 \left(\frac{20}{9000 \times 6}\right) = 0.942 \quad \text{deg}$$

Figure A-9 shows idealized step response characteristics for the same design example when traveling 1.1 deg and 2.75 deg.

SINUSOIDAL MOTION WITH TORQUE AND VELOCITY LIMITING

If the load is moving sinusoidally,

$$\delta = A \sin 2\pi f t \quad \text{deg} \quad \text{(A-22)}$$

$$\omega = \dot{\delta} = 2\pi f A \cos 2\pi f t \quad \text{deg/s} \quad \text{(A-23)}$$

$$\alpha = \dot{\omega} = -4(\pi f)^2 A \sin 2\pi f t \quad \text{deg/s}^2 \quad \text{(A-24)}$$

where A is the amplitude of the load motion in degrees, δ is the load deflection in degrees, ω is the load angular velocity in degrees/second, α is the load angular acceleration in deg/s/s and f is the frequency of the sinusoidal motion in Hertz. If the ratio of motor speed to load speed is G, the peak angular velocity of the motor is

$$\omega_M = \frac{2\pi f G A}{6} \quad \text{r/min} \quad \text{(A-25)}$$

Therefore, if the motor speed can be no greater than N_M (r/min), velocity limiting will occur if the amplitude of the motion exceeds

$$A_V = \frac{3N_M}{\pi G f} \quad \text{deg} \quad \text{(A-26)}$$

Similarly, if the maximum motor torque is T_M (in-lb) and the system inertia reflected to the motor shaft is J (in-lb-s^2), the maximum motor acceleration is

$$\alpha_M = \frac{T_M}{J} \left(\frac{\text{rad}}{\text{sec}^2}\right) \left(\frac{180 \text{ deg}}{\pi \text{ rad}}\right) \quad \frac{\text{deg}}{s^2} \quad \text{(A-27)}$$

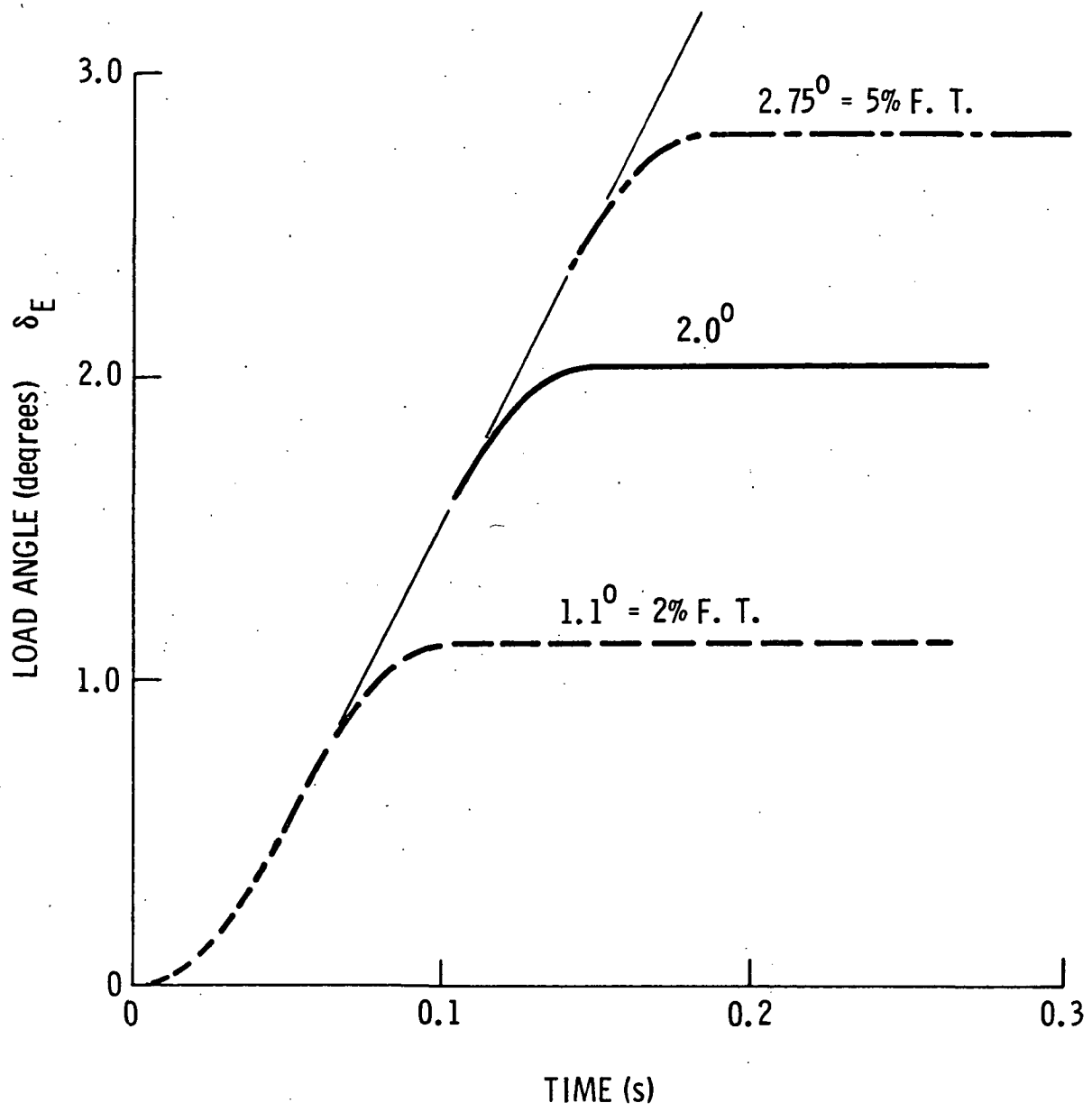

Figure A-9. Step Response with Torque and Velocity Limiting

Therefore, acceleration (torque) limiting will occur if

$$\frac{180\ T_M}{\pi J} = 4\pi^2 f^2 GA \qquad \text{deg/s}^2 \qquad \text{(A-28)}$$

Therefore, the amplitude of the motion which results in acceleration limiting is given by

$$A_A = \frac{45\ T_M}{\pi^3 f^2 GJ} \qquad \text{deg} \qquad \text{(A-29)}$$

For the same design example used above, with

$T_M = 120$ in-lb $\qquad J = 0.006$ in-lb-s^2

$G = 2700 \qquad N_M = 9000$ r/min

$$A_V = \frac{3}{\pi}\frac{(9000)}{(2700)f} = \frac{3.18}{f} \qquad \text{deg}$$

and

$$A_A = \frac{45\ (120)}{\pi^3\ (2700)(0.006)f^2} = \frac{10.75}{f^2} \qquad \text{deg}$$

Figure A-10 shows the velocity and acceleration limits for this design example. For this case, velocity limiting will be encountered before acceleration limiting for frequencies less than 3.4 Hz. At higher frequencies, the motion will be constrained by acceleration limiting.

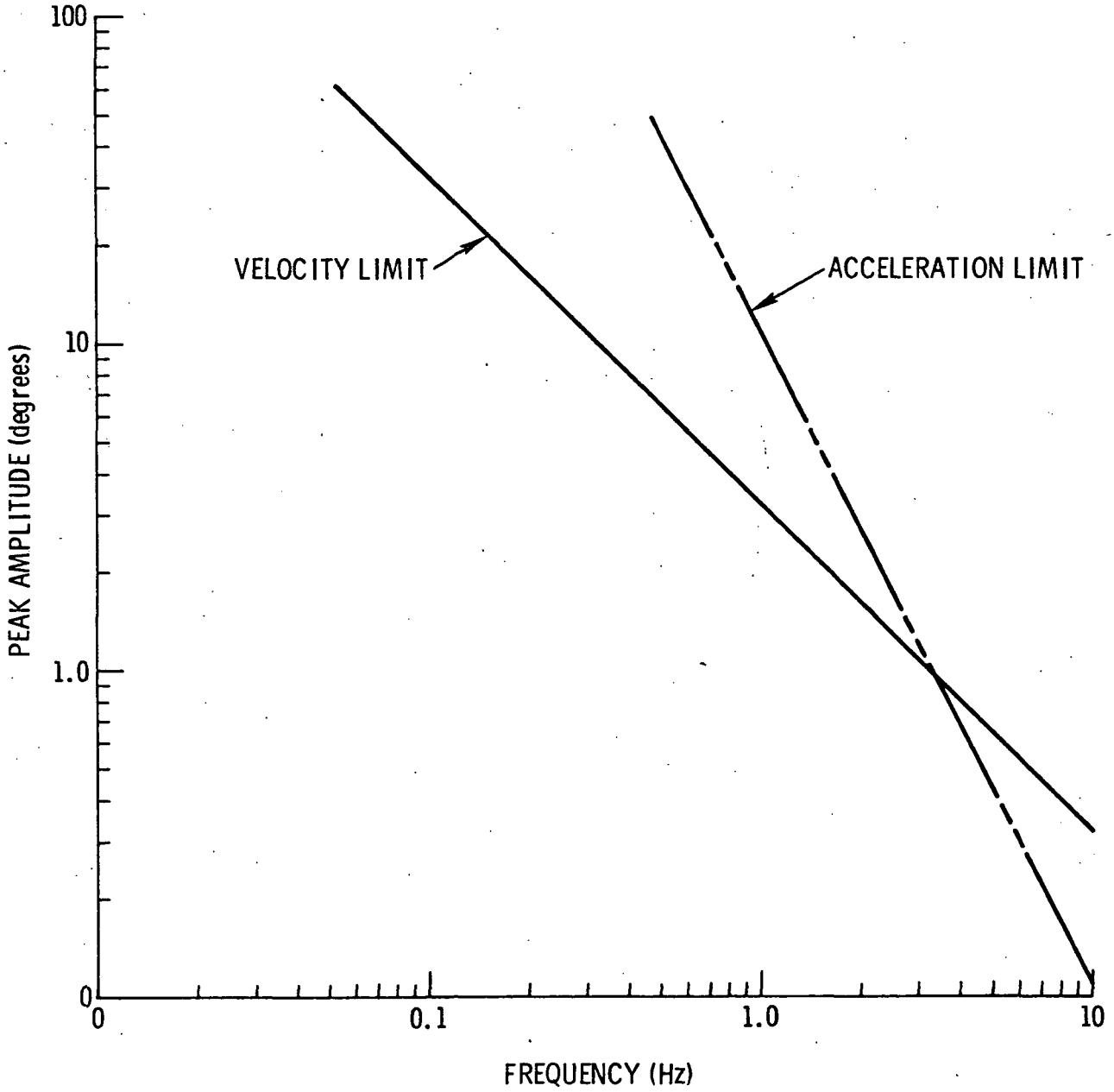

Figure A-10. Limiting Amplitude of Sinusoidal Motion

APPENDIX B
GEAR DESIGN DATA

This Appendix contains detailed design data on the gears used in the differential gearbox.

GLEASON WORKS ROCHESTER, NEW YORK 14603 U.S.A.

Gleason Works

ZEROL BEVEL GEAR DIMENSIONS NO. 474,675 FORM K DATE 10/25/74

R1 Zerol Bevel

Delco Electronics

~~GLEASON WORKS ROCHESTER~~

	PINION	GEAR
NUMBER OF TEETH	16	60
PART NUMBER		
DIAMETRAL PITCH		13,333
FACE WIDTH	0,600"	0,600"
PRESSURE ANGLE	20D 0M	
SHAFT ANGLE	90D 0M	
TRANSVERSE CONTACT RATIO		1,318
FACE CONTACT RATIO		0,000
MODIFIED CONTACT RATIO		1,318
OUTER CONE DISTANCE		2,329"
MEAN CONE DISTANCE		2,029"
PITCH DIAMETER	1,200"	4,500"
CIRCULAR PITCH	0,236"	
WORKING DEPTH	0,150"	
WHOLE DEPTH	0,166"	0,166"
CLEARANCE	0,016"	0,016"
ADDENDUM	0,107"	0,043"
DEDENDUM	0,059"	0,123"

	PINION	GEAR
OUTSIDE DIAMETER	1,407"	4,522"
PITCH APEX TO CROWN	2,222"	0,559"
MEAN CIRCULAR THICKNESS	0,123"	0,078"
OUTER NORMAL TOP LAND	0,033"	0,056"
MEAN NORMAL TOP LAND	0,044"	0,059"
INNER NORMAL TOP LAND	0,055"	0,055"
PITCH ANGLE	14D 56M	75D 4M
FACE ANGLE OF BLANK	19D 33M	78D 7M
ROOT ANGLE	11D 53M	70D 27M
DEDENDUM ANGLE	3D 3M	4D 37M
OUTER SPIRAL ANGLE		5D 22M
MEAN SPIRAL ANGLE		0D 0M
INNER SPIRAL ANGLE		6D 14M
HAND OF SPIRAL	LH	RH
DRIVING MEMBER	PIN	
DIRECTION OF ROTATION-DRIVER	REV	
OUTER NORMAL BACKLASH	MIN 0,002"	MAX 0,004"
TOOTH TAPER	DPLX	
CUTTING METHOD		SB
GEAR TYPE		GENERATED
FACE IN PERCENT OF CONE DIST		25,766

THEORETICAL CUTTER RADIUS				
CUTTER RADIUS	3,000"			
CALC. GEAR FINISH. PT. WIDTH		0,053"		
GEAR FINISHING POINT WIDTH		0,055"		
ROUGHING POINT WIDTH	0,045"	0,055"		
OUTER SLOT WIDTH	0,049"	0,055"		
MEAN SLOT WIDTH	0,049"	0,055"		
INNER SLOT WIDTH	0,046"	0,055"		
FINISHING CUTTER BLADE POINT	0,030"	0,030"		
STOCK ALLOWANCE	0,001"	-0,000"		
MAX. RADIUS-CUTTER BLADES	0,025"	0,031"		
MAX. RADIUS-MUTILATION	0,044"	0,059"		
MAX. RADIUS-INTERFERENCE	0,018"	0,040"		
CUTTER EDGE RADIUS	0,010"	0,010"		
CALC. CUTTER NUMBER	0	0		
MAX. NO. BLADES IN CUTTER		31,285		
CUTTER BLADES REQUIRED	STD DEPTH	STD DEPTH		

GEOMETRY FACTOR-STRENGTH-J		0,1862		0,1631
STRENGTH FACTOR-Q		104,116		31,686
SIZE FACTOR - KS		0,523		
FACTOR	KI	1,5169		
STRENGTH BALANCE DESIRED	STRS			
STRENGTH BALANCE OBTAINED	TPLD			0,100
GEOMETRY FACTOR-DURABILITY-I		0,0597		
DURABILITY FACTOR-Z		17408,63		9093,06
GEOMETRY FACTOR-SCORING-G	*	0,009598		
SCORING FACTOR - X		1,0157		
ROOT LINE FACE WIDTH		0,600"		0,600"
PROFILE SLIDING FACTOR		0,00159		0,00264
RATIO OF INVOLUTE/OUTER CONE		2,019		
AXIAL FACTOR-DRIVER CW	OUT	0,179	OUT	0,179
AXIAL FACTOR-DRIVER CCW	OUT	0,179	OUT	0,179
SEPARATING FACTOR-DRIVER CW	SEP	0,673	SEP	0,048
SEPARATING FACTOR-DRIVER CCW	SEP	0,673	SEP	0,048

GEAR ANGULAR FACE - CONCAVE	11D 12M
GEAR ANGULAR FACE - CONVEX	11D 45M
GEAR ANGULAR FACE - TOTAL	11D 30M

DUPLEX SUM OF DEDENDUM ANG	
ROUGHING RADIAL	3,622"

*THIS FACTOR IS USED IN THE 1966 SCORING FORMULA

RELEASED BY - DRA

ZEROL IS A TRADEMARK OF THE GLEASON WORKS

DELCO ELECTRONICS DIVISION • SANTA BARBARA OPERATIONS • GENERAL MOTORS CORPORATION

GLEASON WORKS ROCHESTER, NEW YORK 14603 U.S.A.

Gleason Works

R2 Bevel Gear

ZEROL BEVEL GEAR DIMENSIONS NO. 474,213 FORM K DATE 8/23/74

CUSTOMER - DELCO ELECTRONICS

	PINION	GEAR
NUMBER OF TEETH	26	39
PART NUMBER		
DIAMETRAL PITCH		9.630
FACE WIDTH	0.630"	0.630"
PRESSURE ANGLE	20° 0'	
SHAFT ANGLE	90° 0'	
TRANSVERSE CONTACT RATIO		1.451
FACE CONTACT RATIO		0.000
MODIFIED CONTACT RATIO		1.451
OUTER CONE DISTANCE		2.438"
MEAN CONE DISTANCE		2.119"
PITCH DIAMETER	2.700"	4.050"
CIRCULAR PITCH	0.326"	
WORKING DEPTH	0.208"	
WHOLE DEPTH	0.229"	0.229"
CLEARANCE	0.022"	0.022"
ADDENDUM	0.130"	0.077"
DEDENDUM	0.099"	0.152"

	PINION		GEAR	
OUTSIDE DIAMETER	2.917"		4.136"	
PITCH APEX TO CROWN	1.953"		1.286"	
MEAN CIRCULAR THICKNESS	0.148"		0.131"	
OUTER NORMAL TOP LAND	0.057"		0.088"	
MEAN NORMAL TOP LAND	0.065"		0.092"	
INNER NORMAL TOP LAND	0.072"		0.087"	
PITCH ANGLE	33° 41'		56° 19'	
FACE ANGLE OF BLANK	39° 20'		60° 42'	
ROOT ANGLE	29° 18'		50° 40'	
DEDENDUM ANGLE	4° 24'		5° 38'	
OUTER SPIRAL ANGLE			5° 38'	
MEAN SPIRAL ANGLE			0° 0'	
INNER SPIRAL ANGLE			- 6° 33'	
HAND OF SPIRAL	LH	RH		
DRIVING MEMBER	PIN			
DIRECTION OF ROTATION-DRIVER	REV			
OUTER NORMAL BACKLASH	MIN	0.003" MAX	0.005"	
TOOTH TAPER	DPLX			
CUTTING METHOD		SB		
GEAR TYPE			GENERATED	
FACE WIDTH IN PERCENT OF CONE DISTANCE			25.837	

	PINION	GEAR
THEORETICAL CUTTER RADIUS		
CUTTER RADIUS	3.000"	
CALC. GEAR FINISH. PT. WIDTH		0.066"
GEAR FINISHING POINT WIDTH		0.065"
ROUGHING POINT WIDTH	0.065"	0.055"
OUTER SLOT WIDTH	0.080"	0.065"
MEAN SLOT WIDTH	0.080"	0.065"
INNER SLOT WIDTH	0.076"	0.065"
FINISHING CUTTER BLADE POINT	0.050"	0.040"
STOCK ALLOWANCE	0.011"	0.010"
MAX. RADIUS-CUTTER BLADES	0.053"	0.039"
MAX. RADIUS-MUTILATION	0.060"	0.059"
MAX. RADIUS-INTERFERENCE	0.026"	0.040"
CUTTER EDGE RADIUS	0.020"	0.020"
CALC. CUTTER NUMBER	0	0
MAX. NO. BLADES IN CUTTER		
CUTTER BLADES REQUIRED	STD DEPTH	STD DEPTH

	PINION		GEAR	
GEOMETRY FACTOR-STRENGTH-J	0.2192		0.2184	
STRENGTH FACTOR-G	29.327		19.424	
SIZE FACTOR - KS	0.568			
FACTOR KI	1.3785			
STRENGTH BALANCE DESIRED STRS				
STRENGTH BALANCE OBTAINED STRS			0.009	
GEOMETRY FACTOR-DURABILITY-I	0.0657			
DURABILITY FACTOR-I	7282.		5946.	
GEOMETRY FACTOR-SCORING-G *	0.004531			
SCORING FACTOR - X	0.5547			
ROOT LINE FACE WIDTH	0.630"		0.630"	
PROFILE SLIDING FACTOR	0.002523		0.002307	
RATIO OF INVOLUTE/OUTER CONE	1.949			
AXIAL FACTOR-DRIVER CW OUT	0.172	OUT	0.172	
AXIAL FACTOR-DRIVER CCW OUT	0.172	OUT	0.172	
SEPARATING FACTOR-DRIVER CW SEP	0.258	SEP	0.115	
SEPARATING FACTOR-DRIVER CCW SEP	0.258	SEP	0.115	

GEAR ANGULAR FACE - CONCAVE
GEAR ANGULAR FACE - CONVEX
GEAR ANGULAR FACE - TOTAL

DUPLEX SUM OF DEDENDUM ANG
ROUGHING RADIAL 3.473"

*THIS FACTOR IS USED IN THE 1966 SCORING FORMULA

RELEASED BY -

"ZEROL" IS A TRADEMARK OF THE GLEASON WORKS

Gleason Works

1ST & 2ND Differential

ZEROL BEVEL GEAR DIMENSIONS NO. 474.200 FORM K DATE 8/26/74

CUSTOMER - DELCO ELECTRONICS

	PINION	GEAR
NUMBER OF TEETH	29	29
PART NUMBER		
DIAMETRAL PITCH		10.357
FACE WIDTH	0.515"	0.515"
PRESSURE ANGLE	20° 0'	
SHAFT ANGLE	90° 0'	
TRANSVERSE CONTACT RATIO		1.477
FACE CONTACT RATIO		0.000
MODIFIED CONTACT RATIO		1.477
OUTER CONE DISTANCE		1.980"
MEAN CONE DISTANCE		1.722"
PITCH DIAMETER	2.800"	2.800"
CIRCULAR PITCH	0.303"	
WORKING DEPTH	0.193"	
WHOLE DEPTH	0.213"	0.213"
CLEARANCE	0.020"	0.020"
ADDENDUM	0.097"	0.097"
DEDENDUM	0.117"	0.117"

		PINION		GEAR
OUTSIDE DIAMETER		2.937"		2.937"
PITCH APEX TO CROWN		1.332"		1.332"
MEAN CIRCULAR THICKNESS		0.133"		0.128"
OUTER NORMAL TOP LAND		0.073"		0.067"
MEAN NORMAL TOP LAND		0.077"		0.072"
INNER NORMAL TOP LAND		0.080"		0.070"
PITCH ANGLE		45° 0'		45° 0'
FACE ANGLE OF BLANK		50° 41'		50° 41'
ROOT ANGLE		39° 19'		39° 19'
DEDENDUM ANGLE		5° 41'		5° 41'
OUTER SPIRAL ANGLE				4° 36'
MEAN SPIRAL ANGLE				0° 0'
INNER SPIRAL ANGLE			-	5° 21'
HAND OF SPIRAL	LH		RH	
DRIVING MEMBER	PIN			
DIRECTION OF ROTATION-DRIVER	REV			
OUTER NORMAL BACKLASH	MIN	0.002"	MAX	0.004"
TOOTH TAPER	DPLY			
CUTTING METHOD			SR	
GEAR TYPE				GENERATED
FACE WIDTH IN PERCENT OF CONE DISTANCE				26.011

THEORETICAL CUTTER RADIUS				
CUTTER RADIUS	3.000"			
CALC. GEAR FINISH. FT. WIDTH		0.068"		
GEAR FINISHING POINT WIDTH		0.070"		
ROUGHING POINT WIDTH	0.050"	0.060"		
OUTER SLOT WIDTH	0.065"	0.070"		
MEA. SLOT WIDTH	0.063"	0.070"		
INNER SLOT WIDTH	0.060"	0.070"		
FINISHING CUTTER BLADE POINT	0.040"	0.040"		
STOCK ALLOWANCE	0.010"	0.010"		
MAX. RADIUS-CUTTER BLADES	0.038"	0.066"		
MAX. RADIUS-MUTILATION	0.050"	0.068"		
MAX. RADIUS-INTERFERENCE	0.030"	0.030"		
CUTTER EDGE RADIUS	0.020"	0.020"		
CALC. CUTTER NUMBER	0	0		
MAX. NO. BLADES IN CUTTER				
CUTTER BLADES REQUIRED	STD DEPTH	STD DEPTH		

GEOMETRY FACTOR-STRENGTH-J		0.2215		0.2215
STRENGTH FACTOR-Q		36.158		36.153
SIZE FACTOR - KS		0.557		
FACTOR	KI	1.3544		
STRENGTH BALANCE DESIRED	STRS			
STRENGTH BALANCE OBTAINED	STRS			
GEOMETRY FACTOR-DURABILITY-I		0.0587		
DURABILITY FACTOR-Z		8219.		8219.
GEOMETRY FACTOR-SCORING-G *		0.003523		
SCORING FACTOR - X		0.5007		
ROOT LINE FACE WIDTH		0.515"		0.515"
PROFILE SLIDING FACTOR		0.002260		0.002260
RATIO OF INVOLUTE/OUTER CONE		2.313		
AXIAL FACTOR-DRIVER CW	OUT	0.211	OUT	0.211
AXIAL FACTOR-DRIVER CCW	OUT	0.211	OUT	0.211
SEPARATING FACTOR-DRIVER CW	SEP	0.211	SEP	0.211
SEPARATING FACTOR-DRIVER CCW	SEP	0.211	SEP	0.211

DUPLEX SUM OF DEDENDUM ANG.
ROUGHING RADIAL 3.459"

*THIS FACTOR IS USED IN THE 1966 SCORING FORMULA

MEAN ANGULAR FACE = CONCAVE
MEAN ANGULAR FACE = CONVEX
MEAN ANGULAR FACE = TOTAL

RELEASED BY -

"ZEROL" IS A REGISTERED TRADEMARK OF THE GLEASON WORKS

GLEASON WORKS ROCHESTER, NEW YORK 14603 U.S.A.

DELCO ELECTRONICS DIVISION • SANTA BARBARA OPERATIONS • GENERAL MOTORS CORPORATION